BULLETIN DE L'ASSOCIATION MINERALOGIQUE DU CANADA

THE CANADIAN MINERALOGIST

JOURNAL OF THE MINERALOGICAL ASSOCIATION OF CANADA

Volume 30 June 1992 Part 2

Canadian Mineralogist
Vol. 30, pp. 249-287 (1992)

A PROTON-MICROPROBE STUDY OF MAGMATIC SULFIDE ORES FROM THE NORIL'SK-TALNAKH DISTRICT, SIBERIA

GERALD K. CZAMANSKE
U.S. Geological Survey, 345 Middlefield Road, Menlo Park, California 94025, U.S.A.

VLADIMIR E. KUNILOV
Noril'sk Nickel State Concern, Gvardeyskaya Square 2, Noril'sk 663300, Russia

MICHAEL L. ZIENTEK
U.S. Geological Survey, U.S. Courthouse, Spokane, Washington 99201, U.S.A.

LOUIS J. CABRI
Canada Centre for Mineral and Energy Technology, 555 Booth Street, Ottawa, Ontario K1A 0G1

ALEXANDER P. LIKHACHEV
Central Research Institute of Geological Prospecting for Base and Precious Metals, Varshavskoye Shosse 129B, Moscow 113545, Russia

LEWIS C. CALK AND ROBERT L. OSCARSON
U.S. Geological Survey, 345 Middlefield Road, Menlo Park, California 94025, U.S.A.

ABSTRACT

Proton and electron microprobes have been used to analyze all major coexisting Cu–Fe–Ni sulfide minerals in a suite of 22 ore samples from the rich Cu–Ni–platinum-group-element deposits of the Noril'sk–Talnakh district, Russia. Simultaneous analyses were obtained with the proton microprobe for 30 elements, ranging in atomic number from ^{26}Fe to ^{83}Bi; for the suite of trace constituents ranging from ^{30}Zn to ^{83}Bi, typical minimum detection levels (MDL) range from 4.5 to 50 ppm. Among the data are some of the first microbeam analyses for low-level, trace-element contents of lamellar cubanite, mooihoekite, talnakhite, mackinawite, godlevskite, and bornite, and the first that reveal the presence of Pd in apparent solid-solution in sulfide phases other than pentlandite. Palladium concentrations range from 12 to 96 ppm for 16 analyses of chalcopyrite in 7 samples, from 7 to 52 ppm for 11 analyses of cubanite in 6 samples, and from 77 to 2,920 ppm for 11 analyses of mackinawite in 4 samples. Platinum, Rh, and Ru are rarely above their MDL in any Cu–Fe–Ni sulfide mineral. Thallium-bearing chalcopyrite and pentlandite are present in several samples. The distribution of Se is remarkably uniform among coexisting sulfide minerals and, surprisingly, only Pd, Zn, and Ga show a consistent preference for a particular mineral. Results of bulk analyses are presented for 20 samples of ore from the enormous, mineralogically zoned Kharaelakhsky orebody of the Kharaelakhsky intrusion and the Medvezhy Creek open-pit mine of the Noril'sk I intrusion. Palladium concentrations in massive sulfide ore range from 10 to 445 ppm, and Pt concentrations, from 1.4 to 215 ppm. Palladium concentrations in pentlandite are related to ore type, not bulk Pd concentration in the ore, Ni/Fe ratio in pentlandite, or sulfur fugacity. Palladium concentrations in pentlandite in massive ores from the Kharaelakhsky orebody range from 68 to 284 ppm in pyrrhotite-bearing ore and from <5 to 14 ppm in Cu-rich, pyrrhotite-free ore; in contrast, they range from 203 to 2540 ppm in three samples of Cu-rich, pyrrhotite-free vein ore from the Medvezhy Creek open pit. The spatial distribution of mineral assemblages, ore textures, bulk-composition data, and experimental studies of the Cu–Fe–Ni–S system indicate that fractional crystallization of monosulfide solid solution (*Mss*) and migration of resultant Cu-rich (20–29 wt.% Cu) sulfide liquids were important processes in the evolution of the Noril'sk–Talnakh ores. These processes gave rise to differences in bulk composition that caused pentlandite to crystallize predominantly from *Mss* in ores that ultimately became pyrrhotite-bearing, and from trace-element-enriched, intermediate solid-solution in ores that ultimately became pyrrhotite-free. Enrichment of the Cu-rich liquids in the suite of trace elements critical to platinum-group-mineral (PGM) crystallization significantly lowered solidus temperatures within those ores. When large amounts of Cu-rich liquid (*e.g.*, parts of the Kharaelakhsky orebody) cooled relatively slowly, both high-temperature crystallization of PGM and migration of Pd to a low-melting, dispersed liquid phase concentrated Pd that might otherwise have entered pentlandite. When the Cu-rich liquid was injected as veins, rapid quenching precluded both processes; minute (typically <5 μm) PGM crystallized within Cu–Fe–Ni sulfide minerals, leaving substantial concentrations of Pd in solid solution in pentlandite. Relatively lower concentrations of Ag, Bi, Cd, Pb, Sb, and Sn in the Cu-rich liquids that crystallized as veins at Medvezhy Creek also may have inhibited high-temperature crystallization of PGM. Weight ratios of (Se/S) $\times$ 10^6 in the ores average 420 and support a predominantly magmatic origin for the ore sulfur.

SOMMAIRE

Nous avons utilisé les microsondes protonique et électronique pour analyser tous les sulfures de Fe–Ni–Cu coexistants dans une suite de vingt-deux échantillons de minerai de Cu–Ni et des éléments du groupe du platine, provenant des gisements de Noril'sk–Talnakh, en Union Soviétique. Des analyses simultanées ont été effectuées par microsonde protonique pour trente éléments, dans l'intervalle de nombre atomique compris entre ^{26}Fe à ^{83}Bi. Pour les éléments traces, allant de ^{30}Zn à ^{83}Bi, les seuils de détection sont typiquement entre 4.5 et 50 ppm. Parmi les données se trouvent les premiers résultats d'analyse par microsonde des teneurs d'oligo-éléments de cubanite lamellaire, talnakhite, mooihoekite, mackinawite, godlevskite, et bornite, ainsi que les premiers qui révèlent la présence de Pd apparemment en solution solide dans les sulfures autres que la pentlandite. Les teneurs en Pd varient entre 12 et 96 ppm dans seize analyses de chalcopyrite provenant de sept échantillons, entre 7 et 52 ppm dans onze analyses de cubanite (6 échantillons), et entre 77 et 2,920 ppm dans onze analyses de mackinawite (4 échantillons). Pour la première fois, nous décrivons la présence de chalcopyrite et pentlandite thallifères dans le minerai. Nous décrivons aussi les compositions globales de vingt échantillons de minerai provenant du vaste gîte de Kharaelakhsky, minéralogiquement zoné, situé dans la complexe intrusif du même nom, et de la mine à ciel ouvert de Medvezhy Creek, dans le complexe de Noril'sk I. Quoique notre étude ne fait qu'ajouter aux données déjà accumulées au cours des études soviétiques de la minéralogie et de la répartition des éléments traces dans le gîte de Kharaelakhsky, des données comparables n'existaient pas pour le minerai de Medvezhy Creek. Là, pentlandite et mackinawite contiennent entre 200 et 2,500 ppm de Pd, beaucoup plus que la teneur de tout échantillon de pentlandite analysé du gîte de Kharaelakhsky. A la lumière des données sur la composition globale des échantillons de minerai et des études expérimentales dans le système Cu–Ni–Fe–S, nous émettons une nouvelle hypothèse à propos du contrôle de la teneur en Pd de la pentlandite. La durée de la trempe et du temps de recuit, ainsi que la présence de *Mss* dans l'assemblage, exerceraient un contrôle plus important sur l'incorporation du Pd en solution solide que le rapport Ni/Fe de la pentlandite ou la fugacité du soufre. Le rapport de (Se/S) $\times$ 10^6 dans les échantillons de minerai est en moyenne 420, et concorde donc avec une origine surtout magmatique pour le soufre qui se trouve dans le minerai.

(Traduit par la Rédaction)

Mots-clés: Noril'sk, Talnakh, microsonde protonique, éléments du groupe du platine, éléments traces, Ni, Cu, Se, Russie.

INTRODUCTION

The opportunity to sample and study ores from the famed Noril'sk–Talnakh deposits of Siberian Russia arose in 1990 through a joint memorandum of understanding between the U.S. Geological Survey and the Ministry of Geology of the USSR. These deposits constitute one of the singular mineralized districts in the world; contained Cu–Ni resources are comparable to those of the deposits at Sudbury, Ontario (in excess of 20 million tonnes of Cu and Ni; DeYoung *et al.* 1985). In addition, the Noril'sk–Talnakh deposits are the largest repository of platinum-group elements aside from the Bushveld Complex, South Africa. In recent years, platinum-group-element production from the Soviet Union is thought to have been roughly equivalent to output from South Africa (Coombes 1991); nearly all of this production is from Noril'sk–Talnakh. These deposits are also unique in their association with a continental-flood-basalt province, in the inordinate amount of massive sulfide found in association with three elongate (15–18 km) mafic–ultramafic intrusions 1 to 3 km wide and less than 350 m thick, and in the exceptionally high concentrations of platinum-group elements (PGE), Cu, and Ni contained in the ores (Table 1).

Although mining of Cu–Ni–PGE ores began in the Noril'sk I intrusion in 1935, less has been published about the mineralogy and geochemistry of those ores than about ores from the Kharaelakhsky and Talnakh orebodies of the Talnakh district, which were not discovered until

TABLE 1. COMPOSITIONS OF REPRESENTATIVE ORE SAMPLES FROM THE OKTYABR'SKY, KOMSOMOLSKY, AND MEDVEZHY CREEK MINES.

	90OMZ S2-3	90OC 12	90OC 6B*	90OC 4	90OC 13	90OC 29	90OC 6A*	90OMZ S1-3	90OC 2**	90OC 5
Ca, wt.%	0.23	0.15	0.09	0.18	0.24	0.24	0.20	<0.01	0.60	<0.02
Fe	54.3	51.2	48.7	47.3	40.0	40.2	39.3	38.9	31.6	35.2
Ni	3.5	3.8	4.5	3.0	1.8	1.8	1.4	2.1	2.1	3.8
Cu	4.02	6.53	8.51	12.5	20.5	21.7	22.3	22.5	26.4	27.1
S	30.0	36.1	33.2	32.2	32.9	33.4	33.3	32.8	27.4	33.0
Co, ppm	1270	1560	1300	970	950	940	390	910	590	780
Zn	280	270	360	440	830	800	670	530	480	710
As	0.57	0.47	1.4	1.3	0.55	0.35	0.45	0.24	8.1	47
Se	58	47	78	76	110	104	72	90	93	197
Ag	<7	17	26	22	33	37	33	30	90	310
Cd	<7	<6	<5	<6	17	15	11	10	20	33
Sn	2.6	2.2	2.7	6.7	20	14	5.3	8.5	15.8	50
Sb	<0.05	0.33	0.09	0.35	0.22	0.52	0.05	<0.05	1.4	4.9
Te	0.27	0.27	0.65	1.4	5.8	4.2	0.65	3.4	7.6	30
Au	0.17	0.43	0.53	0.85	1.5	1.6	1.1	1.9	5.5	17.2
Tl	0.3	0.9	0.2	0.5	0.8	0.9	0.5	0.5	0.5	3.9
Pb	<10	20	10	60	230	190	160	100	240	320
Bi	0.20	0.66	0.96	1.3	4.9	4.1	0.32	1.7	7.2	42
Rh	0.27	0.65	0.11	0.11	0.03	0.07	0.006	0.32	0.04	0.15
Pd	10.8	19.9	19.8	21.5	38.6	39	10.5	29.4	40	119
Pt	1.4	2.9	2.2	4.3	3.0	4.3	4.1	7.5	34	121

	90OC 9	90OC 14	90OMZ S1-1	90OC 1+	90KMZ 5	90MC 10++	90MC 16	90MC 15	90MCZC 1	90MC 5
Ca	<0.01	<0.02	<0.01	7.0	0.14	5.5	<0.02	0.11	<0.02	0.20
Fe	37.0	34.5	35.4	14.4	44.7	11.7	42.1	32.3	30.9	30.5
Ni	2.6	3.5	2.5	0.57	5.0	0.63	8.1	7.1	6.5	6.0
Cu	28.2	28.6	29.0	6.20	3.80	1.04	11.8	24.3	24.9	28.0
S	30.3	33.2	31.5	6.30	32.0	2.80	34.0	34.0	32.9	33.8
Co	660	710	590	210	1380	200	1370	920	730	660
Zn	640	600	770	310	230	140	450	690	580	610
As	2.0	1.2	6.6	0.62	0.94	<0.05	1.9	2.2	10	5.0
Se	148	209	120	16	59	6	141	218	328	241
Ag	130	270	170	20	6	<8	33	66	73	26
Cd	43	52	49	10	<6	<8	<6	8	<6	15
Sn	85	60	40	5.4	0.7	20	2.2	15	25	9.6
Sb	2.0	1.4	2.9	0.38	0.05	0.26	0.12	0.25	1.2	0.29
Te	16	20	10.5	2.7	0.7	1.2	2.8	24	85	38
Au	2.2	5.3	4.4	0.43	0.20	0.32	1.9	11.1	11.4	1.2
Tl	5.0	3.8	2.3	0.4	1.3	0.1	0.2	1.2	8.3	1.2
Pb	790	630	600	240	<10	90	<10	<10	10	<10
Bi	8.2	13	12	2.5	0.28	0.41	1.1	4.5	3.8	7.8
Rh	0.01	0.02	0.02	0.006	0.03	0.39	2.4	0.32	0.04	0.15
Pd	132	149	77	11.6	27.7	7.9	87.3	337	233	445
Pt	22.5	25.6	20.1	1.8	5.3	1.7	65.2	106.4	215	38.5

Major elements in wt.%; minor elements and PGE in ppm; Ca content is an indication of contaminating gangue; low totals also reflect the presence of magnetite.

* 90OC6B is a 1-1.2-cm-thick cpy-rich layer against the footwall beneath 90OC6A, which represents the dominant ore type; ** vein 5-7 cm wide; + disseminated ore; ++ droplet ore.

Analysts: at the U.S. Geological Survey, Fe, Ni, Cu, Co, Zn, Pb-Paul Lamothe by ICP-AES; S-Terry Fries by combustion with IR detection; Ca, Ag, Cd-Paul H. Briggs by ICP-AES; As, Sb-Terry Fries by hydride generation plus AAS; Te, Bi-Sarah Pribble by ion exchange plus graphite-furnace AAS; Sn-Neil Elsheimer by solvent extraction plus graphite furnace AAS; Se-Bi-Shia King by EDXRF; Tl-Leon A. Bradley by flame AAS; at the University of Quebec at Chicoutimi, Au, Rh, Pd, Pt-Sarah-Jane Barnes by NiS fire assay plus INAA.

the 1960s. Perhaps that has been a function of the exceptional zonation in mineral assemblages and the spectacular size of these orebodies. By the early 1970s, Soviet investigators had done an excellent job of documenting most of the dramatic chemical and mineralogical contrasts between the pyrrhotite-rich and the Cu-rich, S-poor (here defined as containing the metal-rich phases mooihoekite and talnakhite) ore assemblages. They knew that the Cu-rich ores are enriched in PGE and other trace elements and, as a result of early electron-microprobe studies, that pentlandite is Ni- and

Pd-rich in pyrrhotite ores and relatively Ni- and Pd-poor in the Cu-rich ores, where Pd typically is concentrated in platinum-group minerals (PGM). They analyzed two or three generations of the more common Cu–Fe–Ni sulfide minerals and carried out experimental studies in an attempt to understand their observations. From study of dozens of PGM (commonly new mineral species), they learned their associations and parageneses; a great deal of this work is summarized by Genkin *et al.* (1981). Literature searches suggest that study of these ores has waned in recent years, and that for some reason the trace-element characteristics of the Noril'sk ores were never as well studied or reported.

This study was undertaken because trace-element concentrations in sulfide minerals and the distribution of trace elements among coexisting sulfide minerals are of great scientific and economic interest. The extensive experimental research reported by M. Makovicky *et al.* (1986, 1988) and E. Makovicky *et al.* (1990) was specifically designed to obtain data on the distribution of PGE among the sulfide minerals that predominate in the Noril'sk–Talnakh ores. These ores may be viewed as retrograde metamorphic rocks that have continued to react at temperatures below 138°C, based on apparent pentlandite equilibration and the maximum temperature for the pyrrhotite + troilite assemblage (neglecting Cu and Ni in solid solution). Thus, the Noril'sk–Talnakh ores provide a natural laboratory for obtaining data concerning processes of low-temperature equilibration and the distribution coefficients of trace elements, data that are difficult to obtain by low-temperature experimentation. From an economic viewpoint, it is of considerable importance to know the concentrations and mineral residency of both valuable and deleterious elements so that ore beneficiation and metallurgical techniques may be optimized.

In view of the stature of these orebodies, the limitations of our sampling, and the effort that has gone on before us, we acknowledge the limitations of this contribution. For the North American authors, it is based on the briefest of introductions to the ores. Our Soviet colleagues, however, have together devoted more than 70 years to the district.

GEOLOGICAL SETTING

The ore deposits of the Noril'sk–Talnakh district are associated with hypabyssal intrusions related to the Siberian flood basalt province (SFBP). The SFBP is one of the world's largest; it is principally exposed in the Tungusska syneclise or basin on the northwestern edge of the Siberian platform, but basalts considered to belong to this province are found in the late Mesozoic fold-and-thrust belt in the Taimyr Peninsula (Milanovskiy 1976, Zonenshain *et al.* 1990, their Fig. 117) and occur in widespread localities beneath the western Siberian lowlands almost as far west as the Ural Mountains (Makarenko 1976, his Fig. 2; Zonenshain *et al.* 1990, their Fig. 179). Relatively continuous exposures of basalt cover a minimum area of 3.4×10^5 km^2; however, if one includes areas where associated mafic intrusions cut underlying strata beyond exposures of basaltic lava, the size of the province increases to about 1.5×10^6 km^2 (Basaltic Volcanism Study Project 1981). Milanovskiy (1976) estimated that rocks associated with early Mesozoic flood basalt magmatism once covered an area of 4×10^6 km^2 in the whole of north-central Siberia and had a volume of $2–3 \times 10^6$ km^3.

Using the ^{40}Ar/^{39}Ar laser age-spectrum technique, Dalrymple *et al.* (1991) determined a closure age of 249 ± 0.8 Ma for biotite from an ore-bearing vein in the Zapolyarny mine of the Noril'sk I intrusion. Subsequently, I.H. Campbell (written commun. 1992) used the SHRIMP ion microprobe at the Australian National University to determine an age of 248 ± 4 Ma on zircon in pegmatoidal taxitic gabbrodolerite from the Medvezky Creek open pit. These ^{40}Ar/^{39}Ar and U–Pb ages are not statistically different from one another or from the age of 251.2 ± 3.4 Ma recently determined for the Permo-Triassic boundary by SHRIMP ion-microprobe analysis of zircon from a bentonite layer in the Chinese stratotype section at Changxing (Claoué-Long *et al.* 1991).

All features of the geological evolution of the Noril'sk area are most compatible with a mantle plume model for the origin of the SFBP. SFBP magmatism took place during the collision of the Kazakhstan and Siberian continents with East Europe, that formed the fold-and-thrust belt of the Urals in the late Permian and early Triassic (270–220 Ma; Zonenshain *et al.* 1990). Makarenko (1976) and L.P. Zonenshain (verbal commun., 1990) noted that rifting took place in middle to late Triassic time, and hundreds of kilometers west of Noril'sk. The Noril'sk–Talnakh district lies at the extreme northwestern corner of both the Siberian platform and the most extensive, relatively undisturbed exposures of the SFBP. Zonenshain *et al.* (1990) emphasized that, within the Siberian platform, the flood basalts were intruded in an extensional environment, but that despite this

FIG. 1. Simplified geological map of the Noril'sk–Talnakh district, showing major structural features and subsurface outlines of the fully differentiated, ore-bearing intrusions (black, true scale): (1) the Talnakh and Kharaelakhsky intrusions; (2) intrusions of the Noril'sk area. (3) Location of the Bolgokhtokhsky granodioritic intrusion.

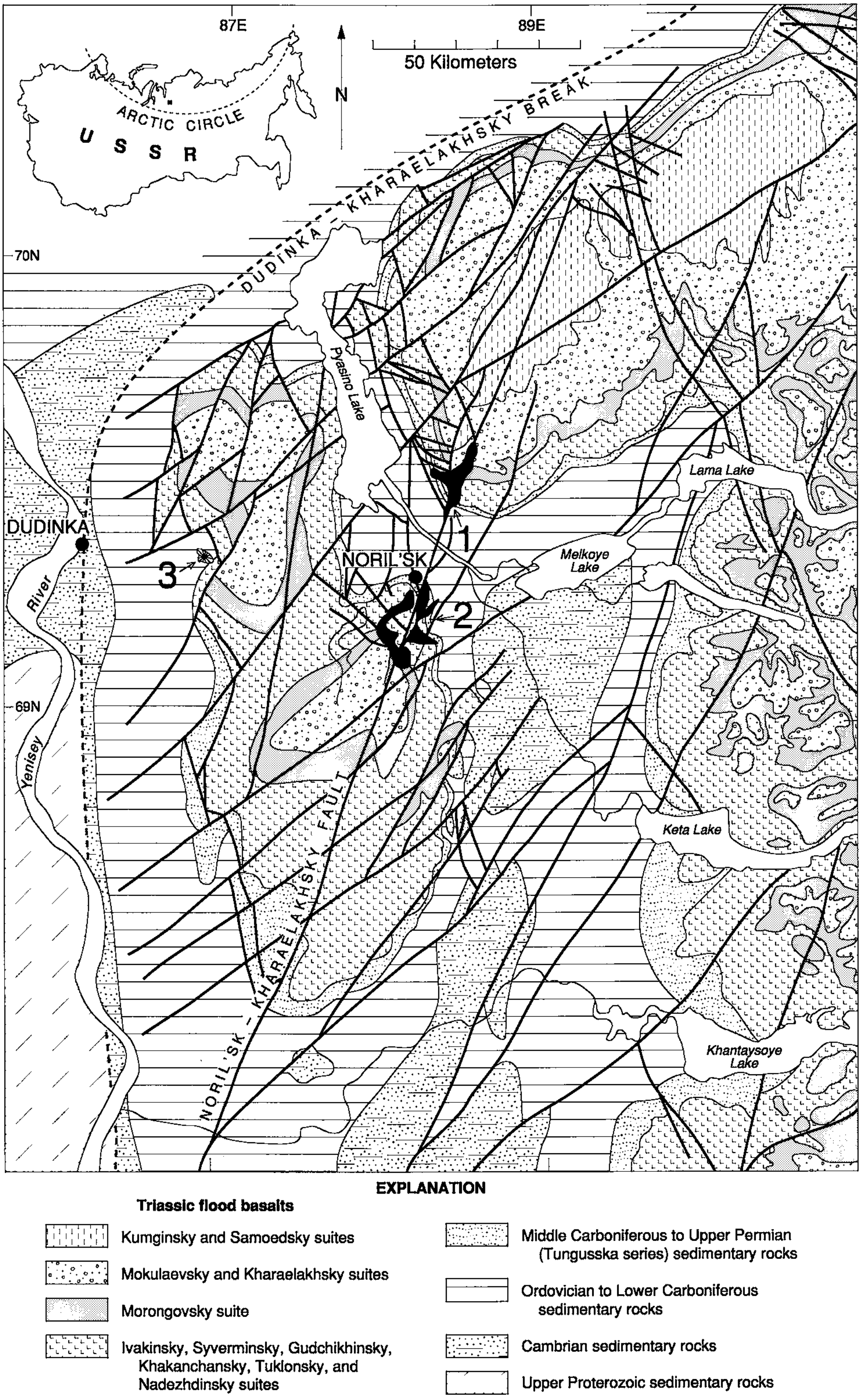
87E
89E
50 Kilometers
N
ARCTIC CIRCLE
U S S R
DUDINKA – KHARAELAKHSKY BREAK
70N
69N
Pyasino Lake
Lama Lake
Melkoye Lake
Keta Lake
Khantaysoye Lake
DUDINKA
NORIL'SK
Yenisey River
1
2
3
NORIL'SK – KHARAELAKHSKY FAULT
EXPLANATION
Triassic flood basalts
Kumginsky and Samoedsky suites
Mokulaevsky and Kharaelakhsky suites
Morongovsky suite
Ivakinsky, Syverminsky, Gudchikhinsky, Khakanchansky, Tuklonsky, and Nadezhdinsky suites
Middle Carboniferous to Upper Permian (Tungusska series) sedimentary rocks
Ordovician to Lower Carboniferous sedimentary rocks
Cambrian sedimentary rocks
Upper Proterozoic sedimentary rocks

extension, crustal thinning (to as little as 8–10 km), and eruption of an enormous volume of flood basalt, there was no major subsidence (*e.g.*, rifting) of the Tungusska region other than isostatic subsidence induced by loading. Deep drilling and reconstructions based on the presence of exposed Precambrian sedimentary rocks 30 km to the west, across the Dudinka–Kharaelakhsky Break (Fig. 1), suggest that Precambrian crystalline rocks lie at a depth of 10 to 12 km in the Noril'sk area, beneath a cover of gently folded Paleozoic and Precambrian sedimentary rocks.

As depicted in Figure 1, the present geological map pattern of the Noril'sk–Talnakh area is dominated by three basalt-filled basins (the Noril'sk, Kharaelakhsky, and Vologochansky depressions). Although it appears that these basins largely represent folds superimposed on once continuous volcanic exposures, deep drilling reveals that the lower suites of the basalt sequence are thickest in these basins, suggesting that they were morphological depressions that developed contemporaneously with volcanism (Fedorenko 1981, Dyuzhikov *et al.* 1988). In contrast to other continental-flood-basalt provinces, SFBP activity in the Noril'sk area was characterized by initial and continuing explosive volcanism. Basaltic tuff units (as much as 45 m thick) constitute about 6.5% of the total basalt sequence in the Noril'sk area (Fedorenko 1981, Fedorenko & Dyuzhikov 1981). Two additional features of the basaltic volcanism are specific to the Noril'sk area and must be considered of great significance with respect to origin of the ore-bearing intrusions and to prospection for such targets in other flood-basalt provinces. First, the lower five basalt suites, best developed in the Noril'sk area, show a broader range of composition (2.7–16.8 wt.% MgO; 24 samples) than can be found in any other region of the SFBP. In contrast, 54 samples of tholeiitic basalt representing the upper 2900 m (six suites) of the flood-basalt sequence have MgO contents within the limited range 6.0–7.6 wt.%. According to Fedorenko (1981), Fedorenko & Dyuzhikov (1981), and Genkin *et al.* (1981), a distinctive feature of early SFBP volcanism in the Noril'sk region was the outpouring of trachybasalts and picritic basalts with tholeiitic basalts. In the axial, deepest parts of the depressions, as much as 150–200 m of picritic basalt may be found. Second, maximal thicknesses of flood basalt, exceeding 3,500 m, are reached in the Noril'sk area, where all eleven suites of the flood-basalt sequence are represented (Fedorenko 1981). Dyuzhikov *et al.* (1988) stated that eruption started earlier and continued for a longer period in the Noril'sk area.

The ore-bearing intrusions of the Noril'sk district lie at the northern margin of the Noril'sk depression, whereas those of the Talnakh district lie at the southern margin of the Kharaelakhsky depression (Fig. 1). The ore-bearing intrusions were typically emplaced near the contact between the base of the SFBP and underlying terrigenous sedimentary rocks; they are cut by the present erosional surface and plunge down-dip, roughly conformably with this contact, toward the deeper, central parts of each depression. Presently, mining is concentrated in the Noril'sk I intrusion, which lies west of the Noril'sk–Kharaelakhsky fault in the Noril'sk district (Fig. 1), and in the Talnakh and Kharaelakhsky intrusions of the Talnakh district, which lie principally east and west of this fault (Fig. 2). The Talnakh intrusion lies in Tungusska series (upper Permian) sedimentary rocks, and the Kharaelakhsky intrusion, in Devonian sedimentary rocks. The Noril'sk I intrusion is partly intrusive into the lower two suites of the basalt sequence,

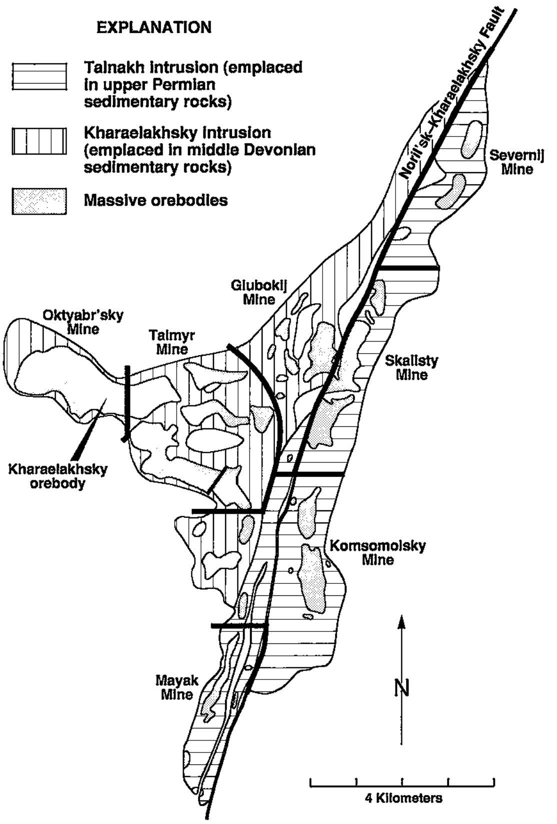

FIG. 2. Cartoon showing subsurface outlines of the fully differentiated, ore-bearing Talnakh and Kharaelakhsky intrusions, locations of massive orebodies at, or beneath, their lower contacts, and mine designations. The Kharaelakhsky orebody is indicated.

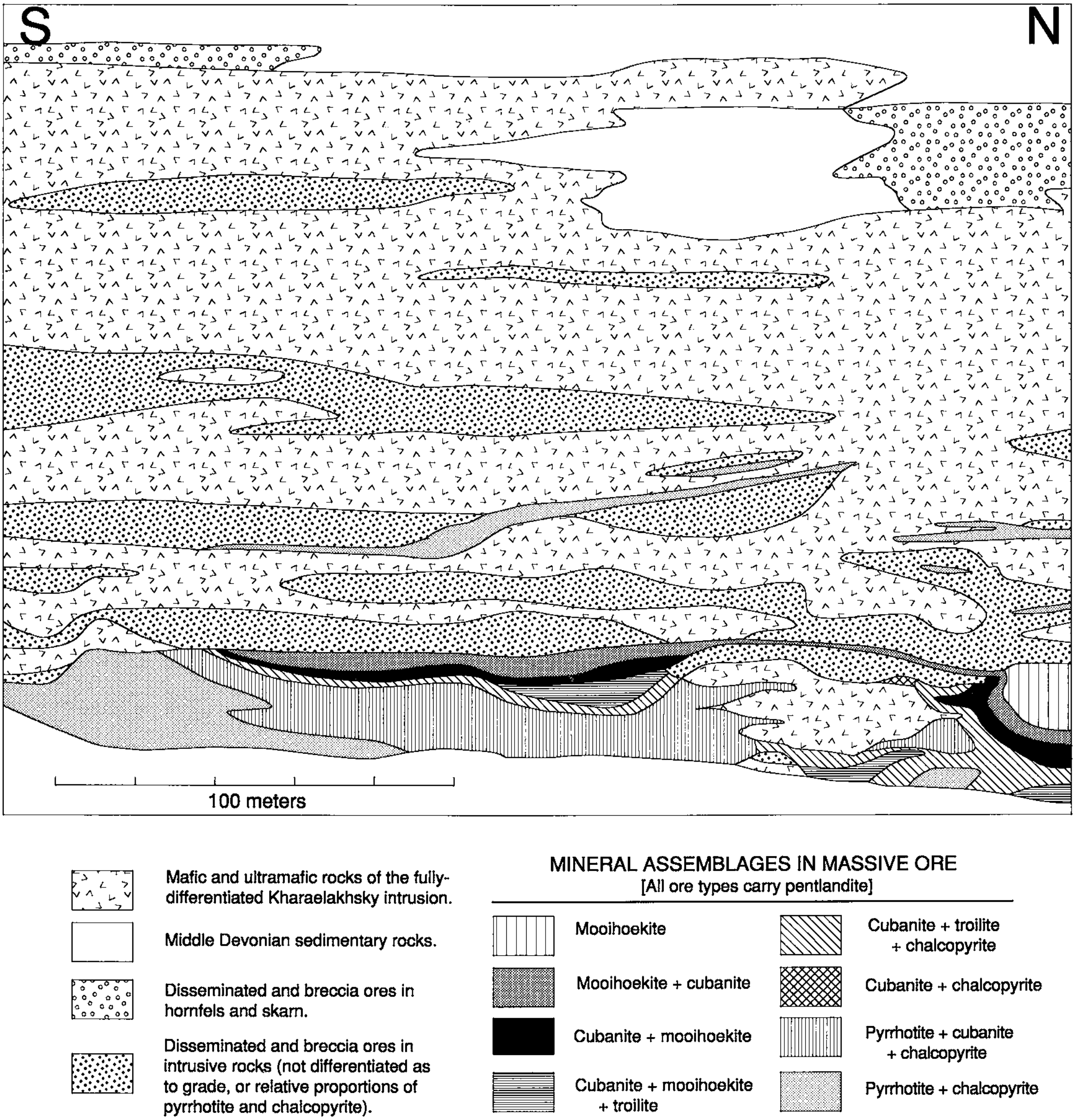

FIG. 3. Vertical S–N section through parts of the Kharaelakhsky intrusion and Kharaelaksky orebody, showing mineral-assemblage zoning in the Oktyabr'sky mine. The stippled pattern for disseminated and breccia sulfide ores indicates zones of enrichment within sulfide-bearing intrusive rocks. Note the discontinuity of these zones of enrichment and the occurrence of massive pyrrhotite-rich ore lenses within the intrusion. Equal vertical and horizontal scales.

and some basalts beneath the intrusion are mineralized.

The ore-bearing intrusions are a special class of nearly a dozen, more abundantly represented groups of intrusions recognized in the Noril'sk area (Fedorenko *et al.* 1984); they form narrow, thin, and elongate, finger-like intrusions. Smirnov (1966) estimated the proportions of their length:breadth:thickness as 120:12:1. In contrast to the myriad of unmineralized, predominantly sill-like intrusions in the district, known through outcrop and drill core, they are also distinguished as being "fully differentiated", *i.e.*, containing a variety of rock types ranging from picrite, through gabbrodolerites containing varying amounts of olivine, to leucogabbro. Indeed, intrusion outlines as typically drawn (*e.g.*, Fig. 2) represent the limits of these finger-like, fully differentiated, intrusions; weakly mineralized, less differentiated sheet-like sills may extend well beyond those limits from lower levels of the fully differentiated ore-bearing intrusions. Petrological and geochemical evidence suggests that the ore-bearing intrusions formed by emplacement of multiple pulses of magma of differing composition, crystallinity, and content of immiscible sulfide liquid. Where hosted in sedimentary strata, the ore-bearing intrusions of the Noril'sk–Talnakh district have produced metamorphic aureoles of seemingly disproportionate thickness.

Disseminated and droplet Cu–Ni–PGE ore is found in contact, taxitic, and picritic gabbrodolerite over nearly the entire areal extent of these rocks in the Noril'sk I, Talnakh, and Kharaelakhsky intrusions. Thus, the stippled pattern of Figure 3, indicating disseminated and breccia ores in intrusive rocks, merely represents zones of relative enrichment in sulfide. In addition, veinlet and breccia ores can be found at the upper and lower contacts of the intrusions. The Noril'sk I intrusion is characterized by almost continuous, relatively flat-lying large veins of massive, pyrrhotite-bearing ore near its lower contact; the veins may occur as sets where depressions cause the intrusion to be thickened. The Talnakh and Kharaelakhsky intrusions are characterized by an abundance of large massive-sulfide orebodies (Fig. 2) that typically occupy depressions along the floor of the intrusion, but in some cases lie below it and are separated from it by a screen of metamorphosed sedimentary rocks.

Exceptional quantities of Cu, Ni, and PGE are contained in the Noril'sk–Talnakh ores. As noted by Genkin *et al.* (1981), even if assimilation of crustal S has significance for these intrusions, the abundance of ore metals within them demands explanation. Based on experimental data for the solubilities of S and PGE in mafic melts, Naldrett (oral commun. 1991) estimated that the amount of sulfide in the Talnakh and Kharaelakhsky intrusions is about 50 times that which can be dissolved in a mafic silicate melt of the volume of the intrusions and that the PGE contents of the ores must have been derived from 300 to 1,800 times more mafic magma than is represented in the intrusions. There seems little question that the richness of Noril'sk deposits is directly related to the availability of vast amounts of basaltic melt from which metals were scavenged in staging chambers in the mantle or in the crust. However, the reasons for the effective concentration of ore metals in the Noril'sk–Talnakh district, and not at other centers of extensive mafic magmatism, are far from obvious, a challenge to understand, and not an appropriate focus for this report. Based on nearly four times as many analyses of mineralized samples, as well as extensive data-sets for the flood basalts and ore-bearing intrusions, these and other issues will be pursued in future contributions.

The fully differentiated, ore-bearing intrusions are represented by Soviet investigators as being "blind" (*i.e.*, having definite boundaries with no exiting channelways), and there appears to be little evidence within the intrusions of large-scale, *in situ* accumulation of sulfides. On the basis of our observations, we believe that the intrusions represent contemporaneous injection of mafic silicate magma laden with immiscible sulfide liquid, and large volumes of nearly pure sulfide liquid. The mechanism for lifting large volumes of sulfide liquid is not readily envisioned, but its operation clearly is not commonplace, and the problem no greater than that of lifting the more dense iron-oxide liquids that form rare, eruptive magnetite flows (*e.g.*, Grez *et al.* 1991). Alternatively, if the intrusions were, in fact, not blind, one might envision the accumulation of dense immiscible sulfide droplets from vast amounts of mafic magma that rose vertically, slowed to traverse the finger-like intrusions, and then rose again to erupt at the surface.

SAMPLING AND METHODOLOGY

This study encompasses only a sampling of the varied ore types of the district. None of the breccia ores or irregular disseminated-ore lenses of the Talnakh and Kharaelakhsky intrusions were sampled. Moreover, the massive orebodies associated with these intrusions do not all show zoning comparable to that of the Kharaelakhsky orebody; some massive orebodies contain mainly pyrrhotite with nonuniform distribution of chalcopyrite, whereas others show partial zoning to cubanite-rich assemblages. Our sampling even falls short of a complete transect through the mineral assemblages of the Kharaelakhsky orebody (Figs. 3, 4); only a few hours were spent underground in the Oktyabr'sky mine, which takes ore from the western part of of this orebody (Fig. 2), and samples from mine stockpiles are only generally located. (Because of inevitable loss of core through assay and spillage, drillcore transects of the orebody are no longer available.) Our sampling of ore types associated with the Noril'sk I intrusion is quite limited, as Genkin (1959) and Smirnov (1966) described many pyrrhotite-bearing ore types from the Noril'sk intrusion and noted that the large veins along the lower part of the intrusion are pyrrhotite-rich. Smirnov estimated the overall proportion of

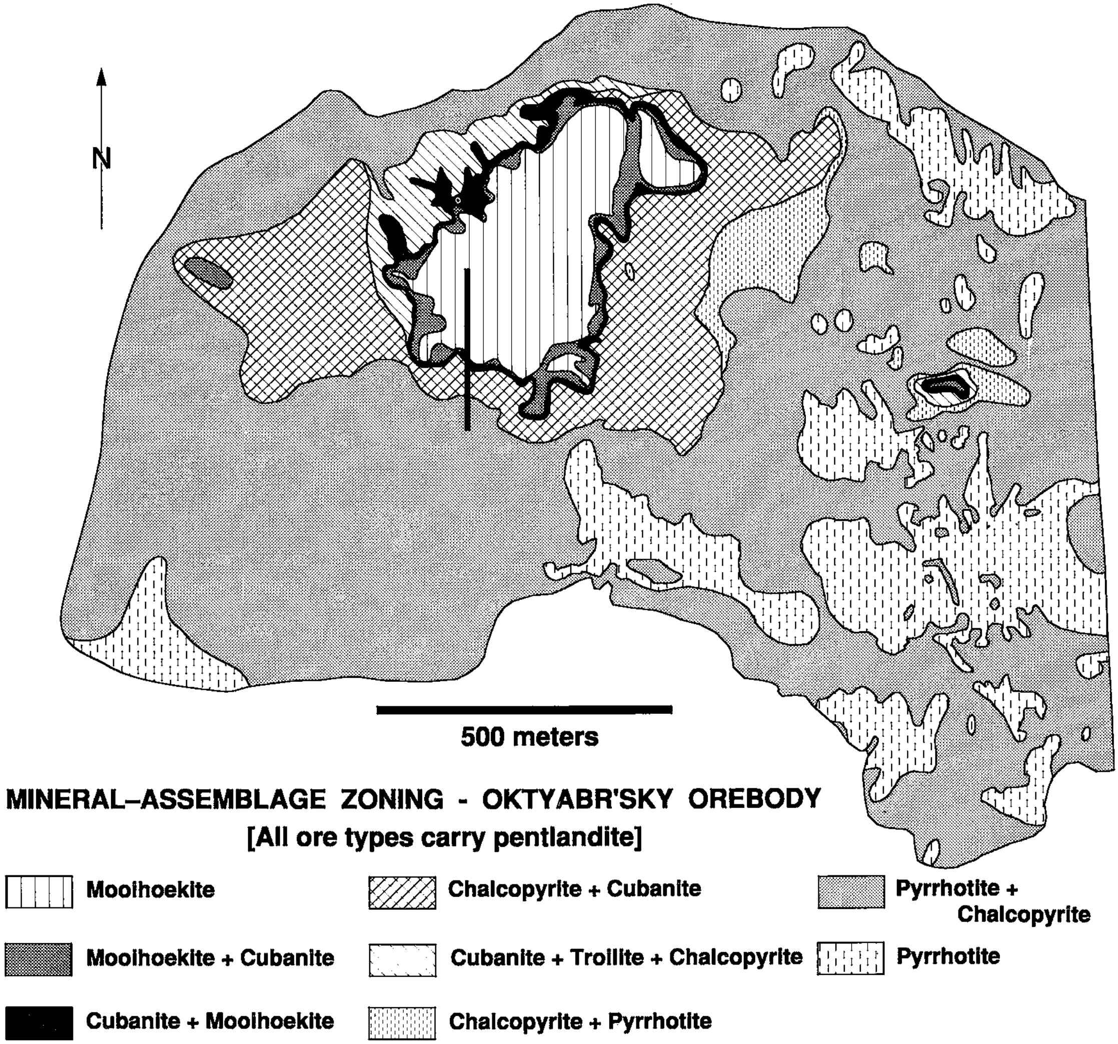

FIG. 4. Plan map of mineral-assemblage zoning in the western part (compare with Fig. 2) of the Kharaelakhsky orebody. Note line of section of Figure 3.

pyrrhotite:chalcopyrite:pentlandite in impregnation ores of the lower differentiates of the intrusion as 5:3:2. Genkin *et al.* (1981) noted that mooihoekite- and talnakhite-bearing assemblages also are found in Noril'sk I ores.

The Medvezhy Creek open-pit mine is elongated N–S and located in the southeastern corner of the northern tip of the Noril'sk I intrusion. Samples (90MC prefixes) were collected from the lower benches and floor of the pit; both droplet ore and massive-sulfide vein fillings (typical widths ≤ 30 cm) are represented. Among the vein ores, three samples (90MC5, 90MC15, 90OMZC1; 24.3–28.0 wt.% Cu) are sometimes specifically classified as "Cu-rich", whereas the fourth (90MC16; 11.6 wt.% Cu) is considered to represent a transitional ore type. Most samples are from the remarkable Kharaelakhsky orebody of the Kharaelakhsky intrusion; this orebody occupies an area of approximately 2.5 km^2. The samples are broadly representative of the mineralogical and compositional zoning within this orebody, as depicted in the vertical section of Figure 3 and the plan view of Figure 4; Cu-rich, S-poor assemblages lie above, as well as inward from, pyrrhotite-rich assemblages. Samples from the Oktyabr'sky mine (90O prefixes) were obtained from both underground workings and ore stockpiles. The stockpile at the No. 1 shaft is composed of mooihoekite- and talnakhite-bearing ore from the Cu-rich, S-poor, upper and central portion of the western part of the mine, whereas that at the No. 2 shaft contains pyrrhotite–chalcopyrite ore from a more easterly part of the mine. Selection of Oktyabr'sky mine samples for proton-microprobe analyses was guided by ore-microscopic examination and bulk-composition data, as reported in Table 1. Thus, distinctive ore assemblages have multiple representation, and confidence in conclusions is enhanced. The Komsomolsky mine works massive orebodies both east and west of the Noril'sk–Kharaelakhsky fault (Fig. 2). Coarse-grained, pyrrhotite–chalcopyrite ore sample 90KMZ5 is from an orebody in Tungusska series sedimentary rocks beneath the Talnakh intrusion on the east side of the fault. Our study also includes three samples obtained from the reference collections of Noril'sk Expedition through the courtesy of Evgenii Sereda; one is of a bornite – chalcopyrite – pentlandite vein and two are of extremely PGE-rich ore that in part consist of a eutectoid-type intergrowth of chalcopyrite and galena. According to Genkin *et al.* (1981), these samples represent the two classic associations of the final stages of ore formation. Because of marked heterogeneity, including the presence of PGM measuring up to 4 mm across, no bulk analyses of these samples were made.

Results of chemical analyses for the sample suite are presented in Table 1, and their essential mineralogy is reported in Appendices I and II. Portions of the samples crushed for splitting and analysis ranged in size from 0.42 to 2.36 kg. Ordering of samples is consistent throughout this report; it is based upon increasing Cu content for massive and vein ores from the Oktyabr'sky and Medvezky Creek mines, with unusual samples placed somewhat arbitrarily, but consistently, in all Tables and Appendices. Studied samples are briefly described in Appendix II; lists of accessory minerals carried in the descriptions are surely incomplete, and in numerous cases stoichiometry is uncertain, as most of the information is based on semiquantitative SEM examination. Extensive Soviet studies of PGM in these ores indicate that full characterization of the PGM in our samples would be laborious and in part peripheral to the central issue of trace-element concentrations in, and distribution among, the major sulfide phases.

Analyses for major and minor elements in pentlandite (pn), pyrrhotite (po), mooihoekite (mh), talnakhite (tk), mackinawite (mk), and godlevskite (gd) (Table 2 and Appendix I) were obtained by electron microprobe at a selection of the same points analyzed by proton microprobe (beam contamination marks were typically visible).

TABLE 2. ELECTRON–MICROPROBE DATA AND ATOMIC PROPORTIONS FOR "MOOIHOEKITE", "TALNAKHITE", MACKINAWITE, GODLEVSKITE, AND Ni–RICH PENTLANDITE

	Cu	Fe	Ni	Co	S	M/S*	Cu/Fe*	Ni/Fe*
"Mooihoekite" (34 atoms)**								
90OC9 (4)+	35.8 8.922	30.9 8.764	0.53 0.143	– –	32.8 16.171	– 1.103	– 1.018	– –
90OMZS1-1 (3)	35.1 8.642	31.2 8.724	0.66 0.176	– –	33.7 16.458	– 1.066	– 0.991	– –
90OC5 (7)	33.8 8.346	30.5 8.548	0.44 0.117	– –	34.8 16.988	– 1.001	– 0.976	– –
"Talnakhite" (33 atoms)								
90OC14 (5)	35.7 8.624	29.6 8.137	0.57 0.149	– –	33.6 16.090	– 1.051	– 1.060	– –
90OMZS1-1 (2)	36.6 8.758	29.7 8.073	1.04 0.269	– –	33.5 15.900	– 1.076	– 1.085	– –
1201 (2)	36.8 8.816	29.0 7.917	0.66 0.171	– –	33.9 16.097	– 1.050	– 1.114	– –
Mackinawite (2 atoms)								
90MC5 (2)	– –	53.9 0.859	8.40 0.127	0.42 0.006	36.4 1.007	– 0.985	– –	– 0.148
90MC15 (3)	– –	54.6 0.866	8.16 0.124	0.46 0.007	36.4 1.003	– 1.000	– –	– 0.143
90MCZC1 (8)	– –	53.8 0.869	7.63 0.117	0.50 0.008	35.8 1.007	– 0.987	– –	– 0.135
90OC21 (7)	– –	55.1 0.882	6.69 0.102	0.73 0.011	36.0 1.005	– 0.990	– –	– 0.116
Godlevskite (13 atoms)								
90OC25 (2)	– –	3.00 0.321	64.3 6.563	0.46 0.047	32.5 6.070	– 1.142	– –	– 20.4
Pentlandite (17 atoms)								
90OC25 (8)	– –	20.0 2.834	44.5 5.992	2.64 0.354	31.7 7.821	– 1.174	– –	– 2.114

* atomic ratios; ** number of atoms assumed in formula; + number of analyses represented by data.
Note: 12 analyses of chalcopyrite in the standard mount and coexisting with "mooihoekite" and "talnakhite" averaged: M/S = 0.996 and Cu/Fe = 0.996. Ideal ratios of 9/8 and 18/16, 17/16, and 7/6 are, respectively 1.125, 1.0625, and 1.1667.

Natural chalcopyrite (cpy) and a series of synthetic Ni- and Co-bearing iron-sulfide phases prepared by G.K.C. were used as standards for the electron-microprobe analyses. Because previous comparisons of electron- and proton-microprobe data for trace elements show that the techniques produce comparable data (*e.g.*, Cabri *et al.* 1984, 1985, Paktunc *et al.* 1990), they are not carefully compared here. Qualitatively, determinations of Ni in pyrrhotite with the proton and electron microprobes are comparable, as reported in Appendix I.

Use of the proton microprobe for analysis of sulfide minerals is now well established (*e.g.*, Cabri *et al.* 1984, 1985, Harris *et al.* 1984, Cabri 1988, Paktunc *et al.* 1990), and the technique so amply described in the literature (*e.g.*, Cabri *et al.* 1984, Campbell & Cookson 1984, Campbell *et al.* 1990) that only the specific operating parameters for the proton microprobe at the University of Guelph will be noted. These were: proton energy, 3 meV; charge, 10 μC; average current, 12–17 nA; counting times, 550–830 s; beam size, 5 × 10 to 6 × 12 μm. A synthetic pyrrhotite standard (in wt.%: Fe 60.93, S 38.87, Se 0.09, Pd 0.11) was used for calibration. Aluminum absorbers 249 and 352 μm thick were used, the former for analyses of pyrrhotite, and the latter for analyses of pentlandite, mackinawite, and the Cu–Fe sulfide minerals. Data reduction, performed with the GUPIX program developed at Guelph (Maxwell *et al.* 1989), was so rapid as to permit examination of results of an analysis before completion of the next analysis.

Comparison of microprobe techniques

Because major-element compositions of Cu–Fe–Ni sulfide minerals in ores and experimental products are also of interest to students of phase assemblages, we report two measures of the ability of the proton microprobe to provide useful data for major elements during the accumulation of trace-element data. The compositions of low-temperature chalcopyrite and cubanite (cb) are stoichiometric at 30.42 wt.% Fe, 34.64 wt.% Cu, and 41.15 wt.% Fe, 23.42 wt.% Cu, respectively. For 53 analyses of chalcopyrite by proton microprobe, Fe content was found to range from 30.27 to 31.81 wt.% (average 30.73 wt.%), and Cu content, to range from 33.78 to 35.55 wt.% (average 34.84 wt.%). Similarly, for 50 analyses of massive and lamellar cubanite, Fe was found to range from 40.22 to 41.95 wt.% (average 41.29 wt.%), and Cu, to range from 23.05 to 24.51 wt.% (average 23.74 wt.%). Whereas these results are, respectively, 0.31 and 0.14 wt.% high for Fe and 0.20 and 0.32 wt.% high for Cu, they compare favorably with what one might expect from a comparable suite of electron-microprobe analyses, and are surely capable of revealing significantly anomalous compositions as, indeed, was the case for "lamellar cubanite" in sample 90OMZS1–1. Comparable analyses were obtained by the electron and proton microprobes for this "cubanite" (Cu, 25.4–25.9; Fe, 39.5–39.9 wt.%), but back-scattered electron images show that its apparent Cu-rich composition is caused by a uniform distribution of irregular elongate bodies (<1 μm wide) of Cu-rich composition (>42 wt.% Cu).

Evaluation of the Fe and Ni data for pentlandite and pyrrhotite is less simple because these minerals are of variable composition, but comparison of proton-microprobe and electron-microprobe data for the same grains is useful. For pentlandite, proton-microprobe values for Ni range from 1.2 wt.% higher to 1.4 wt.% lower than those obtained by electron microprobe, and average just 0.1 wt.% higher; values for Fe range from 0.7 to 2.7 wt.% higher and average 1.6 wt.% higher. For pyrrhotite, the comparison is further complicated by the fact that for four of eleven pyrrhotite-bearing samples, we were able to resolve coexisting troilite and hexagonal pyrrhotite with the electron microprobe but not the proton microprobe. (Note that for this study, we have named pyrrhotite types on the basis of atomic metal/sulfur [M/S] ratios calculated from the electron-microprobe data: monoclinic, 0.858–0.883; hexagonal, 0.909–0.923; and troilite, 0.980–1.003.) Study of the electron- and proton-microprobe data shows that in each of these four samples, the bulk of the pyrrhotite analyzed by proton microprobe is hexagonal pyrrhotite; Fe by proton microprobe averages 1.2 wt.% low (range, 0.67–1.7 wt.% low) compared to the composition determined for hexagonal pyrrhotite in the sample by electron microprobe. In the seven cases where only hexagonal or monoclinic pyrrhotite was identified, proton-microprobe values for Fe range from 0.9 to 1.9 wt.% low and average 1.4 wt.% lower than values obtained by electron microprobe.

RESULTS

In the tradition of Soviet studies, we have paragenetically and chemically characterized the major Cu–Fe–Ni sulfide minerals that were analyzed for trace elements. This information is summarized in Appendices I and II and Table 2. In addition to the electron-microprobe data, the presence of mackinawite, godlevskite, and valleriite was confirmed by X-ray diffraction. Pentlandite was analyzed in all samples except 90OMZS1–1; with two exceptions, the analyzed pentlandite is that termed $\mathrm{Pn_I}$ by Soviet investigators (*e.g.*, Distler *et al.* 1977). This pentlandite is relatively coarse-grained (0.2–2.5 cm across) and equant, albeit in some cases partially replaced by chalcopyrite, cubanite, or bornite (bn). In disseminated ore specimen 90OC1, pentlandite is finer grained, but nonetheless a coherent, major phase. The classic $\mathrm{Pn_{II}}$ of Soviet investigators, pentlandite that exsolved as fine lamellae in pyrrhotite at a low temperature, was analyzed only in sample 90KMZ5 ($\mathrm{Pn_E}$ of Appendix I). Sample 90KMZ5 also contains equant, well-formed pentlandite that forms nearly continuous replacement rims as much as 60 μm thick on chalcopyrite ($\mathrm{Pn_R}$ of Appendix I). As shown by the data of Appendix I, the compositions of these two generations of pentlandite are slightly different. Co content distinguishes two pentlandite compositions in sample 90MC15 (Appendix I). The pentlandite grain containing 0.44 ± 0.01 wt.% Co is 1 cm across and partially altered to mackinawite (Fig. 5), whereas only 0.25 wt.% Co is present in a thin (60 × 1000 μm) lens of pentlandite lying between chalcopyrite and a cubanite lamella. Ni contents of pentlandite correspond both in overall range (26.9–44.5 wt.%) and mineral association with data reported by Genkin *et al.* (1981).

Pyrrhotite was analyzed in all eleven samples in which it is present; in four samples, troilite and hexagonal pyrrhotite in an exsolution relation were analyzed by electron microprobe. All pyrrhotite

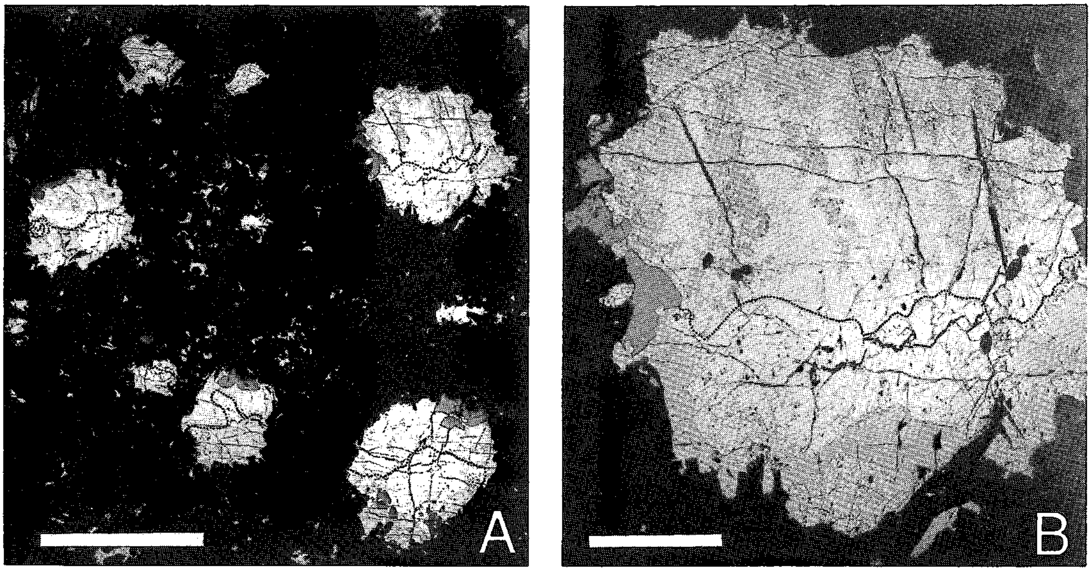

FIG. 5. Reflected-light photomicrographs of droplet-ore sample 90MC10. (A) Typical pattern of droplet distribution. For six droplets, contact representing base of principal mass of former Cu-rich liquid is enhanced by dots. Note anhedral grains of magnetite (dark gray) at margin of each droplet. Bar = 1 cm. (B) Large droplet in upper right of Fig. 5A, again with dot enhancement. Above dots, irregular pyrrhotite (dark) in chalcopyrite host; below dots, intergrown, subequal pyrrhotite (darker) and pentlandite (lighter and fractured). Bar = 2 mm.

analyses except one pertains to relatively coarse pyrrhotite, termed Po_I by Soviet workers, that crystallized from *Mss*. Only the pyrrhotite analyzed in the quenched intermediate solid-solution (*Iss*) component of droplet-ore sample 90MC10 from Medvezhy Creek is Po_{II}, fitting precisely the designation by Genkin *et al.* (1981) as "... fine-grained masses occurring in chalcopyrite in the form of veinlets". Po_{II} is also well developed in sample 90OC13 and the Cu-rich part of sample 90OC6 that crystallized against the footwall, suggesting that the annealing of these samples was incomplete.

Our distinction in Appendix I of lamellar cubanite (cb_L) and massive cubanite (cb_M) corresponds to the designation cb_I and cb_{II} of Genkin *et al.* (1981), who noted that cb_I represents unmixing from *Iss*, and cb_M replaces pyrrhotite, pentlandite, and chalcopyrite-group minerals. All cubanite analyzed is stoichiometric. Electron-microprobe data on "mooihoekite" and "talnakhite" are presented in Table 2. Designation as to one or another of the chalcopyrite-group minerals was based solely on the subjective criterion of near-equal or unequal contents of Fe and Cu; subsequently, formulas were recalculated according to the ideal number of total ions, 34 for "mooihoekite" and 33 for "talnakhite". The credibility of these analytical results may be judged from data reported in the footnote to Table 2 for concurrent analyses of chalcopyrite. (We acknowledge the existence of putoranite and Ni-enriched putoranite in the Noril'sk–Talnakh areas, but elected not to pursue these complex compositional issues.) Fine intergrowths of mooihoekite and talnakhite have been described by Genkin *et al.* (1981) in mooihoekite-rich ores and are characteristic of sample 90OMZS1-1. Low-temperature phase relations in the Cu-rich portion of the Cu-Fe-Ni-S system are extremely complex (*e.g.*, Cabri 1973). Whereas the compositional ranges reported for "mooihoekite" and "talnakhite" in Table 2 are somewhat broader than those reported by Genkin *et al.* (1981), the work of Cabri (1973) suggests that compositional variability in these phases might well be anticipated.

Mackinawite, first reported at Noril'sk by Genkin & Vyal'sov (1967), was analyzed in four samples, in which it replaces pentlandite (Fig. 5). Although not a matter of great consequence, we note that in most respects the determined compositions of mackinawite fall outside the limits cited by Genkin *et al.* (1981), as follows (our ranges follow theirs): Ni, 4.84–6.6 *versus* 6.69–8.40 wt.%; Co, 0.08–0.36 *versus* 0.42–0.73 wt.%; Cu, 0.39–0.96 *versus* 0.02–0.1 wt.%; and M/S (atomic), 0.99–1.11

TABLE 3. SUMMARY OF PROTON-MICROPROBE DATA ACCORDING TO MASSIVE ORE TYPE (PPM)

	Cu/Ni*	Zn	Ga	Se	Pd	Ag	Cd	In	Sn	Te	Pb
OKTYABR'SKY											
Po bearing; Cu, 4.0-22.5 wt.% (7)**											
Pn (7)***	<73-188 (4, 7)++	<42-53 (1, 1)	<35+	45-95 (7, 27)	68-284 (7, 27)	<6	<6	8?-15 (3, 3)	<8-15 (2, 2)	<14-21 (2, 2)	<21-114 (5, 5)
Po (7)	<14-167 (6, 11)	<25	<20	49-90 (7, 23)	<5-6 (1,1)	<6-11 (2, 3)	<6-8 (1, 1)	<7-8? (1, 1)	<8-17 (1, 1)	<13-19 (1, 1)	<14
Cpy (7)	<225	107-558 (7, 25)	<31-50 (6, 9)	50-99 (7, 25)	<6-6? (2, 2?)	<6-10 (3, 7)	<8-17 (7, 14)	<9-11 (1, 1)	<10-18 (5, 8)	<16-30 (3, 3)	<23-295 (5, 13)
Cb (1)	<180	107-636 (1, 6)	<31-50 (1, 3)	81-98 (1, 6)	<6	<6-11 (1, 3)	<6-26 (1, 2)	<8	<10-16 (1, 3)	<15-35 (1, 1)	<23-178 (1, 5)
Po free; Cu, 26.4-29.0 wt.% (5)											
Pn (4)	91-1250 (4, 19)	<44-67 (1, 2)	<35	108-177 (4, 19)	<5-14 (1, 2)	<6-39 (4, 12)	<7-11 (2, 2)	<7	<7-<11	<15-77 (4, 15)	<21-686 (3, 13)
Cpy (1)	<224	79-140 (1-3)	<38-39?	114-120 (1-3)	<6-7 (1, 1)	11-53 (1, 3)	10-23 (1, 3)	9?-18 (1, 2)	<12-18 (1, 1)	<20-30 (1, 1)	306-596 (1, 3)
Cb$_M$ (4)	<175-489 (3, 7)	<46-176 (2, 4)	<32-45 (3, 4)	129-193 (4, 16)	<5-27 (1, 3)	<6-22 (2, 22)	<8-13 (2, 4)	<9-20 (1, 1)	<10-18 (3, 4)	17?-72 (4, 15)	47-407 (3, 14)
Cb$_L$ (4)	<174-9800 (4, 9)	<46-431 (4, 11)	<32-47 (3, 5)	122-230 (4, 14)	<6-7 (1, 2)	15-155 (4, 14)	<8-31 (3, 11)	<9-16 (1, 1)	<11-33 (3, 8)	25-96 (4, 14)	<23-139 (4, 13)
Mh (3)	1900-6350 (3, 11)	<52-114 (2, 4)	<34-53 (3, 8)	128-171 (3, 11)	3.6?-9 (1, 1)	<6-53 (3, 7)	<8-10 (1, 2)	<9-20 (3, 9)	<9-28 (2, 6)	30-52 (2, 9)	<23-151 (3, 9)
Tk (2)	3550-9600 (2, 8)	<53-115 (1, 4)	32?-42 (2, 3)	120-218 (2, 8)	<8	<7-65 (2, 7)	<8-12 (2, 3)	<9-17 (2, 5)	<12-33 (1, 2)	85-128 (1, 6)	<23-66 (2, 5)
MEDVEZHY CREEK; Cu, 11.8-28.0 wt.% (4)											
Pn (4)	<77-1430 (4, 14)	<46-68 (1, 1)	<35	114-345 (4, 17)	203-2540 (4, 17)	<6-112 (4, 15)	<8-16 (1, 2)	<12-28 (2, 3)	<10	<10-380 (4, 16)	<22-70 (2, 3)
Po (1)	17-86 (1, 3)	<25	<20	124-132 (1, 3)	<5	<5	<6	<7	<8	<12-15 (1, 1)	<14
Cpy (4)	<215-8920 (1, 5)	<51-125 (3, 9)	<33-61 (3, 7)	126-356 (4, 15)	<6-35 (4, 9)	8-108 (4, 15)	<7-13 (3, 6)	<9-17 (3, 4)	<10-12 (1, 1)	<15-360 (4, 13)	<21
Cb$_M$ (1)	308, 436 (1, 2)	<46-88 (1, 1)	<32-36 (1, 1)	117-124 (1, 2)	<5	39-58 (1, 2)	8?-9?	<9	<9	<15	<23
Cb$_L$ (3)	174-630 (3, 9)	62-609 (3, 10)	<31-40 (3, 3)	114-362 (3, 10)	<5-50 (3, 5)	13-159 (3, 10)	<8-35 (3, 7)	7?-11 (3, 4)	<10-19 (1, 2)	<14-360 (3, 8)	<23
Mk (3)	68?-1170 (3, 6)	<43-57 (1, 1)	<20	209-383 (3, 9)	310-2920 (3, 9)	8-206 (3, 9)	6?-11 (2, 3)	<12-28 (2, 2)	<8-14 (1, 2)	32-384 (3, 9)	<21-88 (2, 3)

* Cu concentrations in pn, po, and mk, and Ni concentrations in cpy, cb, tk, and mh; ** ore type; range in Cu content and number of samples included; *** number of samples in which mineral was analyzed; + all analyses below indicated MDL; ++ in (x, y), "x" represents the number of samples in which "y" determinations were judged to be legitimately above the MDL.

Note: Samples 90OC1, 90KMZ5, 90MC10, 839, 90OC21 and 90OC25 of Appendix I are not included in this summarization.

versus 0.985-1.000. The cluster of godlevskite grains identified in bornite-rich sample 90OC25 fits perfectly the type description of the mineral in Noril'sk-Talnakh ores (Kulagov *et al.* 1969) in terms of mineral association, paragenesis, and Co-rich composition; as large as 15 × 40 μm, the godlevskite grains are also of typical size (Genkin *et al.* 1981). Genkin *et al.* indicated that godlevskite from the Noril'sk-Talnakh district is Co-bearing and that all godlevskite contains somewhat less metal than required by 7/6 stoichiometry. The godlevskite in sample 90OC25 contains 3.0 wt.% Co, as compared to values of 0.56 and 1.69 wt.% reported by Genkin *et al.*, and shows a slight deficiency in metal.

On the belief that no summary or statistical treatment could well represent our data set, involving analyses of 10 minerals for 30 elements in 22 samples, we have presented virtually all of our analytical data as Appendix I. Results are discussed largely by mineral type in this section of the paper. To facilitate this discussion, summary Table 3 has been prepared according to three ore types, pyrrhotite-bearing and pyrrhotite-free massive ore from the Kharaelakhsky orebody, and Medvezhy Creek vein ore (note that six samples for which data are reported in Appendix I do not fall within these categories.) This choice of ore types is unique to this contribution; the mineral-assemblage classification of Figures 3 and 4 is used by Soviet geologists. The simplistic breakdown of Kharaelakhsky ore types into "pyrrhotite-bearing" and "pyrrhotite-free" arose directly from the distinction between the two ore types with respect to the Pd content of pentlandite, which is considered to reflect a fundamental difference in the crystallization history of pentlandite from sulfide liquids of distinct bulk composition. Minimum levels of detection (MDL) for the trace elements sought are presented in Table 4. Table 3 shows not only the number of samples analyzed from the three main ore types and the number of these that contain each sulfide mineral, but also a quickly assimilated indication of how often a trace element is found in each mineral. Because Se is ubiquitous, the second number below the range of Se concentration values for a given mineral is equal to the total number of spot analyses of that mineral for the given ore type; because the second number under the range of concentration values for each other trace element indicates the number of times the trace element was detected in the given mineral in the ore type, one can compare these two numbers and quickly determine the percentage of measurements in which the trace element was detected (see also Table 3 footnote).

TABLE 4. TYPICAL MINIMUM LEVELS OF DETECTION (MDL) FOR TRACE ELEMENTS IN Ni–Fe–Cu SULFIDE MINERALS BY PROTON–MICROPROBE ANALYSIS (ppm)

	Pentlandite	Pyrrhotite	Chalcopyrite*	Cubanite
Co**	2,500	2,600	2,200	2,700-2,800
Ni	135-210	21-23	220	170-180
Cu	73-80	13-34	130	55-150
Zn	42-45	25	50-54	46-49
Ga	34-36	20	31-40	32-35
Ge	9	5	9	9
As	8-10	4	7-13	6-13
Se	6	4	6	6
Nb	5	3	5	5
Mo	4	4	5	5
Ru	5	4	5	5
Rh	5	4	5	4
Pd	5-6	5	5-6	6
Ag	6	5-6	6-7	6
Cd	6-7	6-8	7-8	5-8
In	7-10	7	8-10	8-9
Sn	8-11	8-9	9-11	9-11
Sb	10-12	10-11	12	12
Te	10-17	11-13	9-16	15-17
Re	38-40	22-23	42-43	39-41
Pt	36	18	45	40
Au	30	17	35	32
Hg	26	16	30	26
Tl	25	18	26	26
Pb	21-23	14	21-31	23
Bi	20	14	22	20

* includes "mooihoekite" and "talnakhite."
** filtering not optimized for low-level Co determinations.

In distilling the data of Appendix I, we have attempted to carefully constrain summary Table 3 to include only measurements that appear to represent true structural incorporation (solid solution) of the trace elements of concern into each mineral; all uniquely anomalous values and all values where coupled high concentrations seem apparent have been excluded from the table. Whether the data of Table 3 are acceptable as measures of solid solution may be judged by the reader, and may vary from case to case. Whether it is important that they be so accepted will clearly depend on the use to be made of the data.

Pentlandite $(Ni,Fe)_9S_8$

Pentlandite is nearly ubiquitous in the Noril'sk–Talnakh ores and was analyzed for major and trace elements in every sample but one (in which it is also present). As documented in numerous Soviet reports, the Ni content of pentlandite in the district is highly variable; in our samples Ni/Fe ratios range from 0.66 to 2.11. Distler *et al.* (1977) suggested that the Pd content of pentlandite is related to its Ni/Fe ratio, but we show later that this relation may be largely an artifact of mixed sample populations. As shown by Table 3, the Pd content of pentlandite is strongly controlled by ore type. Pentlandite in only one sample of pyrrhotite-free Oktyabr'sky ore has minimal Pd content (14 ppm), whereas pentlandite in the pyrrhotite-bearing ore always contains from 68 to 284 ppm Pd. Similarly, only pentlandite in sample 90OC12 from the Oktyabr'sky mine contains as much Pd as is contained in every analyzed sample from Medvezhy Creek. Selenium is a ubiquitous trace element in all analyzed sulfide minerals and is uniformly distributed among them at concentration levels that vary from sample to sample (Table 1); concentrations are lowest in pentlandite in pyrrhotite-bearing ores of the Oktyabr'sky and Komsomolsky mines and highest in ores from Medvezhy Creek. Copper is a significant trace constituent in Noril'sk–Talnakh pentlandite, with 30 determinations between 200 and 720 ppm and 7 values of 900–5,400 ppm; it is below the MDL in pentlandite only in samples of Cu-rich, pyrrhotite-bearing ore from the Oktyabr'sky mine. The data reflect extensive loss of Cu during low-temperature re-equilibration, as it has been shown experimentally that pentlandite in ores of this bulk composition would contain about 2 at.% Cu at 600°C (Hill 1984).

Argentopentlandite [$Ag(Fe,Ni)_8S_8$] was not observed in our study; Ag contents of 10 to 80 ppm are rather erratically found in pentlandite in all ore types. Tellurium contents of pentlandite are comparable to those of associated sulfide minerals and vary appreciably among samples, *e.g.*, from below the MDL in most samples of pyrrhotite-bearing Oktyabr'sky ore to an average of more than 300 ppm in sample 90MCZC1. Lead appears to be an erratic trace constituent of pentlandite in a variety of Oktyabr'sky ore types; it is most abundant in disseminated-ore sample 90OC1 and vein sample 90OC2, but also present in pyrrhotite-bearing sample 90OC29, pyrrhotite-free sample 90OC5, and the PGE-rich samples that contain chalcopyrite–galena intergrowths (839, 90OC21). Among all phases analyzed, Pt was found to be above the MDL only for two analyses of pentlandite replacing chalcopyrite in sample 90KMZ5 from the Komsomolsky mine; this pentlandite also contains as much as 10 ppm Rh. This sample is unique to our sample set in the occurrence of pentlandite as replacement borders on chalcopyrite and in containing well-formed, cubic pyrite in thin, gangue-filled fractures. We have no explanation for the detected Pt and Rh in this pentlandite, but consideration must be given to the possible influence of atypically high sulfur fugacity and the fact that this pentlandite may have formed concurrently with pyrite at temperatures below 212° ± 13°C (Vaughan & Craig 1978). Rhodium and Ru are also present at levels of 20–30 and 7–14 ppm, respectively, in pentlandite in droplet-ore sample 90MC10 from Medvezhy Creek. Thallium, reported here for one of the first times as a trace constituent in Cu–Fe–Ni sulfide minerals, is present in pentlandite in PGE-rich samples 839 and 90OC21. Zinc, Ga, Cd, In, and Sn are infrequent trace constituents of pentlandite.

Pyrrhotite $(Fe,Ni)_{1-x}S$

In notable contrast to pentlandite, minor Pd (5–6 ppm) was found in only 2 of 39 pyrrhotite grains analyzed. Where they coexist, pyrrhotite and pentlandite always have comparable Se contents. Pyrrhotite commonly carries 50 to 250 ppm Cu in solid solution, and the Cu contents of coexisting pyrrhotite and pentlandite commonly are similar. However, in the most Cu-poor sample of massive Oktyabr'sky ore (90OMZS2-3), the Cu content of pyrrhotite is below the MDL, and that of pentlandite near 100 ppm, whereas in the most Cu-rich samples of pyrrhotite-bearing ore, pyrrhotite may contain Cu but pentlandite does not. In droplet-ore sample 90MC10 from Medvezhy Creek, the pyrrhotite that has exsolved from the *Iss* and is complexly intergrown with chalcopyrite in the upper part of each droplet has a consistently high Cu content in comparison to the more typical Cu content of the coherent, large grains of pyrrhotite that exsolved from the *Mss* (Fig. 5; later we discuss this unusual ore texture more fully). In general, our data for Ni, Co, and Cu concentrations in pyrrhotite (Appendix I) agree with the findings of Shishkin *et al.* (1974). Intergrown hexagonal pyrrhotite and troilite contain comparable amounts of Co. The remaining trace elements are all below their MDL in pyrrhotite, except in the sample of Medvezhy Creek droplet ore (90MC10) and in PGE-rich specimen 839. Zinc, Ag, Cd, and Te are notably enriched in the chalcopyrite-hosted pyrrhotite of sample 90MC10; they, like Cu, apparently were residually concentrated, first in the *Iss* and then in pyrrhotite, after rejection by early-crystallized *Mss*. A late stage of ore deposition may be responsible for the incorporation of notably elevated amounts of Ag, Sn, Te, and Pb in the pyrrhotite of sample 839, taken from a cross-cutting vein (see Appendix II). Note that this sample also contains Tl-bearing pentlandite and chalcopyrite, and is the only sample studied in which pyrrhotite and Pd-free pentlandite coexist. Rhodium is present just above the MDL (4 ppm) in pyrrhotite in samples 90OC29 and 90MC16 and at the 11–12 ppm level in the coarsely crystalline pyrrhotite after *Mss* in sample 90MC10. This is less than half the average Rh content of pentlandite in this sample of droplet ore. This result is at variance with the conclusion of Distler *et al.* (1974) that Rh concentrations in pyrrhotite and pentlandite are equal. Ruthenium is at the MDL in sample 90OMZS1-3, but 14–21 ppm Ru are present in pyrrhotite in sample 90OC29.

Chalcopyrite $CuFeS_2$

In all samples from the Oktyabr'sky mine (except sample 90OC1, of disseminated ore in contact gabbrodolerite) and the three samples of Cu-rich Medvezhy Creek vein ore, chalcopyrite contains less than 220 ppm Ni (the MDL). Nickel contents range from 250–370 ppm in chalcopyrite in sample 90OC1, and are comparable in the chalcopyrite of sample 839 and bornite-rich sample 90OC25. Unusually high contents of Ni (2,750–26,100 ppm) were measured in chalcopyrite in samples 90MC10 and 90MC16 from Medvezhy Creek. For sample 90MC10, the relatively rapid quenching evidenced by the inability of the *Iss* to clear itself of pyrrhotite, appears also to have left Ni either in chalcopyrite or in submicroscopic pentlandite grains scattered in chalcopyrite. An entirely opposite proposal may be appropriate for sample 90MC16, insofar as textures in this sample strongly suggest extensive replacement of pentlandite by chalcopyrite. During this process, chalcopyrite may be unable to quantitatively exclude Ni or, perhaps, submicroscopic residual domains of pentlandite. This study demonstrates the solubility of as much as 800 ppm Zn in chalcopyrite, with the highest contents found in the pyrrhotite-bearing Oktyabr'sky ores and in the intergrown chalcopyrite of sample 90MC10. As highlighted by a portion of the bold italicized data of Appendix I, unusually elevated Zn and Cd contents appear to be correlated. In no case did follow-up SEM study reveal the presence of a discrete phase; either micro-inclusions of (Zn,Cd)S lay beneath the polished surface, or we have detected a concentration stage prior to crystallization of (Zn,Cd)S inclusions. Although concentrations are low, it appears that at Medvezhy Creek, Cd is likely to be more concentrated in chalcopyrite than massive cubanite; the highest concentrations are found in lamellar cubanite. Palladium contents of chalcopyrite are generally at the MDL, except in Medvezhy Creek vein ore and in disseminated-ore sample 90OC1, PGE-rich sample 90OC21, and bornite-rich sample 90OC25 from the Oktyabr'sky mine. For four samples of Medvezhy Creek ore, nine determinations of Pd in chalcopyrite range from 12 to 43 ppm, with no apparent relation to content of another trace element. Similarly, 18, 22, and 23 ppm Pd were detected in chalcopyrite in samples 90OC21 and 90OC25, and 12, 30, 34, and 96 ppm Pd in chalcopyrite in sample 90OC1. Gallium is commonly present at detectable levels in chalcopyrite in pyrrhotite-bearing Oktyabr'sky ore, in Medvezhy Creek vein ore, and in samples 90OC21 and 90OC25. Typically, Ag is below or near the MDL (6–7 ppm) in chalcopyrite; however, in samples 839 and 90OC21, as well as all Medvezhy Creek samples, chalcopyrite may contain 23–108 ppm Ag. There is no particular pattern for In and Sn concentrations, which are below or near the MDL in chalcopyrite except for disseminated-ore sample 90OC1 (Sn 9, 25, 43 ppm) and sample 839 (Sn 308, 431 ppm). Tellurium is below or near the MDL in chalcopyrite, except in Medvezhy Creek ore and atypical samples 839, 90OC21, and 90OC25. In these samples, its concentration is comparable to that in coexisting pentlandite, pyrrhotite, cubanite, and mackinawite, ranging from 30 to more than 300 ppm. Lead contents in chalcopyrite are below the MDL in all Medvezhy Creek vein ore, but are appreciable in sample 90OC21 and several samples from the Oktyabr'sky mine. Galena is a major phase in samples 839 and 90OC21, and has been identified as a trace constituent in most Oktyabr'sky ore samples. There is no apparent pattern to the erratic and sometimes high (average 150–400 ppm) Pb contents of some Oktyabr'sky chalcopyrite. As much as 45 ppm Tl was found in chalcopyrite in samples 839 and 90OC21.

Cubanite $CuFe_2S_3$

Where present, cubanite ranges in significance from a minor to a major phase. It is always found in association with pentlandite, and found in association with pyrrhotite in only four of the samples studied. Although cubanite and chalcopyrite are commonly associated in the Noril'sk–Talnakh ores, this association is only found in the Medvezhy Creek ores of our sample suite. Although it has not been possible in every case to characterize analyzed cubanite as lamellar or "so-called" massive, we attempted to do so, based on early indications of trace-element distinctions between the two forms in some samples from the Oktyabr'sky mine. Where coexisting with more massive cubanite, lamellar cubanite may contain higher concentrations of Ni, Zn, Ag, Cd, and Sn. This pattern, best evidenced in samples 90OC5, 90OC9, and 90OC14, must relate (for all but Ni) to a greater acceptance of these elements in the cubanite structure than in the structures of "mooihoekite" or "talnakhite" from which the cubanite lamellae exsolved.

The Ni contents of cubanite are generally comparable to those of coexisting chalcopyrite, but may be lesser or greater. Whereas a single value of 5,240 ppm Ni, obtained for lamellar cubanite in sample 90MC16, might be ascribed to a pentlandite inclusion, it is less easy to dismiss the values of 2465 ppm in sample 90OC5, and 3,000, 9,800, and 16,400 ppm found in sample 90OC9. The "mooihoekite" and "talnakhite" from which cubanite has exsolved in samples 90OC5, 90OC9, 90OC14, and 90OMZS1-1 contain 5,000 to 10,000 ppm Ni as a minor constituent (Table 2, Appendix I). As particular care was taken in locating spots for analysis on cubanite lamellae, the erratic, high Ni contents of the lamellar cubanite exsolved from "mooihoekite" and "talnakhite" would appear to reflect the fact that Ni was relatively inert during the exsolution process. Zinc contents of cubanite are generally less than 200 ppm, and Cd contents less than 12 ppm. Where higher values were obtained, these elements appear coupled; the best example is the regular increase in both Cd and Zn contents in massive cubanite in sample 90OC14. We suspect the presence of submicroscopic concentrations of (Zn,Cd)S similar to larger, but still microscopic, Cd-rich sphalerite grains and stars identified in the ores with the SEM. Cubanite commonly contains Ga in the 35–50 ppm range typical for the other Cu–Fe sulfide minerals. Selenium contents are in all cases commensurate with those of coexisting minerals. Massive cubanite in sample 90OC5 contains 6–27 ppm Pd that does not appear coupled with another trace element; cubanite in Medvezhy Creek ore may contain as much as 50 ppm Pd, as does lamellar cubanite in sample 90OC21. Abnormal concentrations of Pd in lamellar cubanite of sample 90OC5 clearly relate to a submicroscopic association of Pd with Sn. As evidenced in Table 3, cubanite is an important carrier of Ag in Noril'sk and Talnakh ores; invariably, Ag contents are higher in the lamellar variety, where concentrations may reach 150 ppm. Indium is erratically above the MDL in cubanite, as is Sn in Medvezhy Creek ore. In all of the Oktyabr'sky ores in which cubanite was analyzed, Sn is present at the level of 15–18 ppm. Lamellar cubanite may contain 17–37 ppm Sn in Oktyabr'sky ores, and cubanite contains 124 and 231 ppm Sn in sample 839. Concentrations of Te in cubanite are typically comparable to those in associated sulfides, but notably lower for cubanite in samples 90OC10 and 839 and for massive cubanite in sample 90MC16. Lead is below the MDL in Medvezhy Creek cubanite, but typically present in cubanite from the Oktyabr'sky mine; sample 90OC21 contains the most Pb, 542 and 880 ppm. In contrast to other elements, Pb appears to be less concentrated in lamellar cubanite than in massive cubanite in samples 90OC5 and 90OC14. Although cubanite in sample 90OMZS1-3 typically contains 70–200 ppm Pb, Pb is below the MDL in coexisting chalcopyrite. In samples 839 and 90OC21, chalcopyrite contains as much as 45 ppm Tl, whereas Tl is below the MDL of 25–28 ppm in cubanite. In sample 90OMZS1-1, cubanite may contain 14–25 ppm Sb.

"Mooihoekite" $Cu_9Fe_9S_{16}$

Based on electron-microprobe data (Table 2), three pyrrhotite-free samples from the Oktyabr'sky mine are considered to contain "mooihoekite". In contrast to chalcopyrite and cubanite, "mooihoekite" and "talnakhite" contain Ni as a minor rather than a trace constituent (Table 2, Appendix I). Trace-element contents are comparable for "mooihoekite" in samples 90OC5 and 90OC9, but somewhat lower in sample 90OMZS1-1, in which "mooihoekite" and "talnakhite" are finely intergrown. In the latter sample, trace-element concentrations in "mooihoekite", "talnakhite", and lamellar and massive cubanite are generally comparable. Perhaps the only noteworthy differences are the fact that Sn is present in the two types of cubanite, but not in "mooihoekite" and "talnakhite", and only lamellar cubanite contains Zn. Antimony is present (14, 26 ppm) in "mooihoekite" and lamellar cubanite in sample 90OMZS1-1. "Mooihoekite" does not appear to carry Pd, whereas cubanite does in sample 90OC5. Zinc is present in the "mooihoekite" of samples 90OC5 and 90OC9 at levels (60–114 ppm) comparable to those found in associated cubanite, except that lamellar cubanite in sample 90OC5 may contain 300–400 ppm Zn. From 38 to 53 ppm Ga is present in the "mooihoekite" of these two samples, concentrations comparable to those in cubanite in sample 90OC5. Cadmium is somewhat less abundant, and In more abundant, in "mooihoekite" than in coexisting cubanite. The Ag content of "mooihoekite" is comparable to that of cubanite in sample 90OC5, but notably less than that of lamellar cubanite in sample 90OC9. Contents of Se, Sn, Te, and Pb are comparable (at different concentration levels) for "mooihoekite" and cubanite in these two samples.

"Talnakhite" $Cu_9Fe_8S_{16}$

"Talnakhite" was analyzed by electron microprobe in three samples, two of which were studied by proton microprobe (1201 is a reference sample from the collection of Noril'sk Expedition). As a coarse-grained, dominant phase, the "talnakhite" of sample 90OC14 contains much higher concentrations of trace elements than the exsolved "talnakhite" of sample 90OMZS1-1. In sample 90OC14, Zn concentrations in "talnakhite" are comparable to those in lamellar cubanite and less than those in massive cubanite, whereas the opposite is true for Cd. Gallium, Se, and Pb appear to be equally distributed among the three phases. Palladium exceeds the MDL of 6–8 ppm only where an association with Sn is apparent. Silver and Sn are as abundant in "talnakhite" as in lamellar cubanite; both phases carry more Ag and Sn than massive cubanite. Indium (11–17 ppm) and Te (85–128 ppm) appear to prefer the "talnakhite" structure.

Mackinawite $(Fe,Ni)_{1-x}S$

The presence of mackinawite as an alteration product in pentlandite (Fig. 6) has been confirmed by electron-microprobe and X-ray analysis in three samples of Medvezhy Creek vein ore and in sample 90OC21; nickel contents range from 6.69 to 8.40

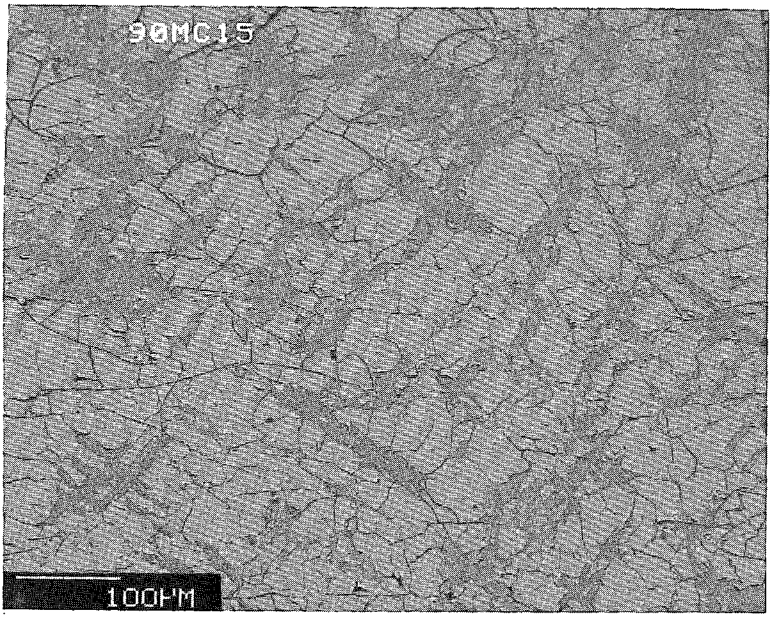

FIG. 6. Representative back-scattered electron image of replacement of Pd-bearing pentlandite by Pd-bearing mackinawite (sample 90MC15).

wt.% (Table 2). The Pd contents of mackinawite are extremely high, exceeding those measured in coexisting pentlandite in two of the four samples. This result suggests that Pd is relatively immobile or even concentrated during the alteration process. Copper is consistently present in mackinawite, often at concentrations greater than 400 ppm, whereas Zn concentrations are negligible. Copper concentrations in mackinawite may be greater than those in the host pentlandite, suggesting that Cu, like Pd, may become more concentrated in this alteration mineral. In all samples, Se, Te, and Pb contents in mackinawite are comparable to those in coexisting sulfide minerals. Silver contents are generally comparable to those in pentlandite, but greater than those found in pentlandite for one analysis of mackinawite in sample 90MC5 and all three analyses of mackinawite in sample 90OC21. Mackinawite in sample 90MC5 contains a trace amount of Sn, and that in sample 90OC21 is enriched in Sn (72–205 ppm) compared to coexisting pentlandite. Gallium and Cd concentrations are at or below their MDL. Mackinawite in sample 90OC21 contains more Tl (105–235 ppm) than any coexisting mineral other than pentlandite.

Bornite Cu_5FeS_4

Bornite, found only in sample 90OC25, was found to be extremely unstable under the proton beam at the high currents employed, and this required rastering of the sample. Its apparent contents of Se (75 ppm), Pd (19 ppm), In (16 ppm), and Te (26 ppm) are comparable to those in coexisting chalcopyrite. Only Ag (65 ppm) appears to be preferentially concentrated in bornite.

Godlevskite $(Ni,Fe)_7S_6$

Godlevskite was identified by electron-microprobe and X-ray analysis in the association of its initial discovery (Kulagov *et al.* 1969), a late-stage bornite–chalcopyrite–pentlandite vein above the Kharaelakhsky orebody. Most trace elements are below their MDL in godlevskite, but it contains a significant amount of Cu (944–1,746 ppm) and has a Se content comparable to that of coexisting sulfide minerals. One spot analysis gave high contents of Pd (19 ppm), Ag (11 ppm), and In (13 ppm).

Magnetite Fe_3O_4

Early crystallization of magnetite is to be expected from magmatic sulfide liquids (Craig & Kullerud 1969, Naldrett 1969). Magnetite is abundant in pyrrhotite-rich ores, abundant to sparse in Cu-rich Kharaelakhsky ores, and rare in the Medvezhy Creek vein ores, although subhedral grains <2 mm across may be found along vein margins. Complex and intriguing textures, noted by Genkin *et al.* (1981) and only hinted at in the descriptions of Appendix II, suggest that a study of magnetite would be of interest. Owing to time limitations, only four grains of magnetite were analyzed in two samples of pyrrhotite-bearing Oktyabr'sky ore, with the following, comparable results (ppm): sample 90OC12: Ni 916, Zn 127, Zr 26, Sn 11; sample 90OC29: Ni 1058, 1107, 1110, Zn 165, 152, 170, Zr 22, 12, 22, Sn 36, 48, 38.

Atypical samples

Sample 90OC1, consisting of disseminated ore in contact gabbrodolerite from the upper contact of the Kharaelakhsky orebody, merits separate consideration on several counts. Perhaps the most striking is that the Pd content of chalcopyrite in this specimen is the highest measured (12–96 ppm), whereas that in pentlandite is below the MDL of 5–6 ppm, as is typical of pyrrhotite-free ore. Chalcopyrite in this specimen and in the quite dissimilar specimen 839 is the only chalcopyrite from the Oktyabr'sky mine that contains Ni well above the MDL of ~220 ppm; it also contains, on average, more Sn (16?–43 ppm) than any sample other than sample 839. Finally, the Te contents of the coexisting pentlandite (29–35 ppm) and chalcopyrite (<15 ppm) are unusually different. We can only suggest that these distinctions result from quenching and isolation of the sulfide component in this disseminated-ore sample, as no comparable sample of this ore type was studied.

The trace-element geochemistry of the major sulfide phases in samples 839 and 90OC21 is unusual. Sample 839 represents a sulfide vein cutting massive sulfide ore in the upper part of the Kharaelahksky orebody, and sample 90OC21 may be comparable. Both samples are enriched in Ag, Au, and PGE, and both contain galena (gal$_I$ of Soviet geologists) in complex intergrowth with chalcopyrite. The samples contain Tl well above the MDL (~26 ppm) in pentlandite, chalcopyrite, and mackinawite. In ores of this type, djerfisherite [$K_6(Cu,Fe,Ni)_{25}S_{26}Cl$] and thalcusite [$Tl_2(Cu,Fe)_4S_4$; Kovalenker *et al.* 1976] are not uncommon (Genkin *et al.* 1981), and the phase $Pd_4Bi_5Cl_3$ has been described (Karpenkov *et al.* 1981). The presence of Tl, K, and Cl, and unexpected irregularities in trace-element concentrations in major sulfide minerals, may relate to the origin of this late-stage ore type as a liquid in equilibrium with solid *Iss* (see Discussion), and possible involvement of hydrothermal solutions. Unusually high concentrations of Ag in the pyrrhotite (222, 367 ppm) of sample 839 and the mackinawite (539, 643, 984 ppm) of 90OC21 are notable, as are uniquely high Sn contents in all analyzed phases of both samples, except for pentlandite in sample 839. The most striking features relate to sample 839; the Pd content of pentlandite in this pyrrhotite-bearing ore is less than the MDL, and the average Se content of cubanite in the sample is only 25 ppm in comparison to an average concentration of 268 ppm Se for 6 analyses of coexisting sulfide minerals. The Te content of this cubanite is also much lower than that of the coexisting phases. We have found no comparable divergences in any other sample. Other notable differences between the two samples are: (1) in addition to Pd, the concentrations of Cu, Zn, Ga, and Sn are below their MDL in the pentlandite of sample 839; (2) chalcopyrite in sample 839 contains at least twice as much Ni as that in sample 90OC21, and contains 4–5 times as much Ag and 3–30 times as much Sn, but only one tenth as much Pb; (3) the lamellar cubanite of sample 90OC21 contains less Zn than any other analyzed lamellar cubanite, remarkably more Pd and Pb, and much less Sn than the cubanite of sample 839.

Other trace elements

Of the other elements sought during our study, only Nb, Mo, Hg, and Bi were never detected near or below their MDL, or if so, as a rare value 2–3 times the MDL, which could be readily ascribed to an inclusion. The following is an inventory of the less commonly detected elements (with their overall MDL) and the fraction of times they were reported as constituents of the major Cu–Fe–Ni sulfide minerals by the Guelph deconvolution program: As (MDL, 4–13 ppm): chalcopyrite (11/52), cubanite (11/53), pyrrhotite (2/39), pentlandite (2/90), "mooihoekite" (2/11), "talnakhite" (2/8), bornite (1/1); Au (17–35 ppm): pyrrhotite (3/39), chalcopyrite (2/52), cubanite (2/53), pentlandite (1/90), "mooihoekite" (1/11); Ge (5–9 ppm): pentlandite (4/90), "mooihoekite" (2/11), cubanite (1/53); Pt (18–45 ppm): pyrrhotite (5/39), pentlandite (3/90); Re (22–43 ppm): pentlandite (5/90), cubanite (3/53), chalcopyrite (2/52), "mooihoekite" (2/11). Rare Au and Pt values 2–3 times their MDL presumably record the presence of inclusions of the Pt minerals and electrum present in these ores.

DISCUSSION

Distribution coefficients

Bethke & Barton (1971) raised the hope that if clean mineral separates of contemporaneous phases could be accurately analyzed, the distribution of minor elements among the phases could allow estimation of temperatures of ore formation. Unavailable at that time, the proton microprobe is ideally suited to provide the quality of analysis required, even for complex growth-zoning in sulfide minerals. Surprisingly, for most trace elements sought, our data reveal little preference among the structures of pyrrhotite, pentlandite, mackinawite, cubanite, and the chalcopyrite-group minerals.

Bethke & Barton (1971) studied the distribution of Cd, Mn, and Se between galena and sphalerite and of Se between galena and chalcopyrite. It seems possible that the strong functions of distribution coefficients with temperature found for these trace elements were largely a function of the galena structure. In fact, Bethke & Barton used their data to calculate distribution coefficients for Se between sphalerite and chalcopyrite (which share the zinc-blende structure), and found that the distribution coefficient decreases with temperature at a rate so slight as to preclude use in geothermometry.

We believe the samples studied from the Noril'sk deposits typically represent equilibration at quite low temperatures. If the most useful distribution coefficients for geothermometry will be those that increase with decreasing temperature, our data eliminate numerous mineral pairs from potential use as geothermometers in the sense proposed by Bethke & Barton. For most substituting trace elements, there appears to be little difference in site preference among the mineral hosts. Of all the elements studied, only Pd, Zn, and Ga show a consistent preference for a particular host; Pd prefers pentlandite and mackinawite, whereas Zn and Ga prefer cubanite and the chalcopyrite-group minerals. High Zn content in the pyrrhotite hosted by chalcopyrite in the droplets of sample 90MC10 is corroborating evidence of arrested equilibration in the droplets. The remarkable uniformity of Se distribution among coexisting minerals has been noted; where distinctly above its MDL, Te is almost as uniformly distributed, whether it be at the 30–80 ppm level (sample 90MC15) or the 260–380 ppm level (sample 90MCZC1). The distribution of Ag is quite erratic, perhaps owing to the fact that it is monovalent and enters into coupled substitutions with trivalent elements; in any given sample, it may be detectable in one or another mineral. Notable are its relatively high concentration in mackinawite in sample 90OC21 (540–980 ppm) and in pyrrhotite in sample 839 (220–360 ppm), as well as its typically low concentration (<60 ppm) in pentlandite, considering the fact that one structural site can be filled with Ag in argentopentlandite [$Ag(Fe,Ni)_8S_8$]. Always near its MDL, In is uniformly distributed in sample 90MCZC1, but appears to favor the pentlandite structure in pyrrhotite-bearing ores and the chalcopyrite-group minerals in pyrrhotite-free ores. Where near its MDL, Sn seems to have no favorite site, as is the case at higher concentrations in sample 90OC21. In other samples, higher concentrations of Sn are commonly found in cubanite and chalcopyrite-group minerals. Concentrations of Pb appear to follow a somewhat consistent, but capricious pattern. Lead is present in pyrrhotite only in galena-bearing sample 839, in which far more Pb was detected in pyrrhotite than in coexisting sulfide minerals. In the pyrrhotite-bearing ores from the Oktyabr'sky mine, Pb is generally more abundant in cubanite or chalcopyrite-group minerals than in pentlandite. Though typically near its MDL, Pb is most commonly detected in pentlandite or mackinawite in the Cu-rich vein ores of Medvezhy Creek. Finally, in disseminated ore sample 90OC1, in sample 90OC21, and in several samples of pyrrhotite-free ore from the Oktyabr'sky mine, Pb is at high levels of concentration in most sulfide phases.

Crystallization paths for sulfide liquid

The spatial distribution of mineral assemblages (Figs. 3, 4), bulk-composition data, and experimental studies of the Cu–Fe–Ni–S system (*e.g.*, Craig & Kullerud 1969) indicate that the Kharaelakhsky orebody represents an enormous pool of sulfide liquid that fractionated by high-temperature crystallization of *Mss* to produce a Cu-rich residual liquid and, ultimately, Cu-rich, pyrrhotite-free ore assemblages complementary to pyrrhotite – chalcopyrite – pentlandite ores. The Cu-rich Medvezhy Creek vein ores are interpreted as injections of comparable Cu-rich differentiates.

On a vastly different scale, ore textures in specimen 90MC10 (Fig. 5), consisting of classic droplet ore in picritic–taxitic gabbrodolerite from the Medvezhy Creek open-pit mine, provide insight into this process and reflect intermediate stages in the crystallization of the immiscible sulfide liquid. Trace-element concentrations and distributions in this ore type are interpreted as antecedent to those represented in the mineral assemblages of the Kharaelakhsky orebody and the Cu-rich veins at Medvezhy Creek. The gabbrodoleritic units of the intrusions that host droplet ore also commonly contain abundant biotite, suggesting that the ore-bearing magmas were relatively volatile-rich and may have had relatively low solidus temperatures for their mafic compositions; *Mss* undoubtedly was crystallizing concurrently with the silicates of the host intrusion. Margins to the solidified droplets are highly irregular, with interfingering sulfide and subhedral silicate crystals, and droplets were commonly deformed. A chalcopyrite-rich assemblage typically occupies the part of each droplet that was uppermost as the rock solidified. The monoclinic pyrrhotite (Po_M of Appendix I) and pentlandite that lie in the lowermost part of each droplet are coarse-grained relative to the chalcopyrite-rich assemblage; contacts between these two minerals range from smooth to complexly interdigitating. (Relative proportions of pyrrhotite and pentlandite and of these minerals relative to the chalcopyrite-rich assemblage vary with the plane of the section.) The coarse-grained pyrrhotite contains both simple and complex exsolution lamellae of pentlandite, and the pentlandite may contain sparse, irregular residues(?) of pyrrhotite. Irregular to well-crystallized pentlandite and pyrrhotite may form a thin rim on one another along contacts with the chalcopyrite-rich assemblage. This latter assemblage constitutes an extremely irregular intergrowth of monoclinic pyrrhotite in chalcopyrite (Po_I and Cpy_I of Appendix I) that also may contain fine exsolution-lamellae of cubanite. A small part of each droplet may consist of pyrrhotite-free chalcopyrite (Cpy_M of Appendix I). Anhedral magnetite grains, as much as several millimeters across, are typically found along an edge of each droplet (Fig. 5).

The findings of Craig *et al.* (1968), Craig & Kullerud (1969), Kullerud *et al.* (1969), and Hill (1984) provide a basis for discussion of the observed mineral relationships in the quenched droplets. With cooling, Ni-bearing *Mss* began to crystallize at a temperature of about 1000°C and sank; the remaining, displaced liquid became increasingly Cu-rich until a temperature of about 850°C was reached. *Iss* may have begun to crystallize from this liquid at about 900°C (Dutrizac 1976), and it is likely that the droplets were solid at 800°C. Data in Table 1 for Cu-rich massive and vein ore suggest that the Cu-rich liquid contained 2.5 to 7.1 wt.% Ni and was enriched in most trace elements. At temperatures below 610°C, pentlandite began to nucleate against and within the crystalline, solidified *Mss*. As the system cooled further, chalcopyrite crystallized from the *Iss*, and Ni released by this reaction migrated along with Ni being released from the *Mss* to augment pentlandite. Traces of Ni not released at higher temperatures formed pentlandite exsolution lamellae in the monoclinic pyrrhotite produced by the breakdown of *Mss*. Sulfur released by crystallization of pentlandite from *Mss* in the droplets may have stabilized this relatively S-rich monoclinic pyrrhotite. The lower-density, Cu-rich liquid that rose to the upper part of the droplets and crystallized as *Iss* is now represented by an extremely intricate intergrowth of irregular fine pyrrhotite veinlets in chalcopyrite. This assemblage and texture contrast notably with those in Cu-rich massive and vein ores, which crystallized from liquids that were removed from *Mss*-rich assemblages; in those ores, pyrrhotite is absent, and pentlandite and chalcopyrite-group minerals resulting from breakdown of *Iss* have segregated to form homogeneous coarse grains.

Because of the isolation and more rapid quenching(?) of the droplets, as well as the presence of pyrrhotite in the assemblage, elemental partitioning in sample 90MC10 contrasts with that measured in the Cu-rich Medvezhy Creek vein ores. Compared to pentlandite in these vein ores, pentlandite in sample 90OC10 is poorer in Ni and richer in Co; it is the only analyzed pentlandite that contains Rh and Ru well above their MDL (<5, 17, 21, 27, 28 and <5, 5, 7, 7, 14 ppm, respectively). Similarly, only the coarse-grained monoclinic pyrrhotite that exsolved from the *Mss* contains detectable Rh (11, 12, 12 ppm). Experimental studies by Distler *et al.* (1977) showed that both Rh and Ru are strongly concentrated in the early-formed *Mss*, but the studies of Makovicky *et al.* (1986) showed that at 900°C, the solubility of Rh in pyrrhotite is far greater than that of Ru. The data of Makovicky *et al.* (1986) for 500°C show marked decreases in the solubilities of both Rh and Ru in pyrrhotite, and our data suggest that Rh and Ru leave the *Mss* and remain concentrated in pentlandite relative to pyrrhotite at intermediate stages of annealing. The coarse-grained pyrrhotite in sample 90MC10 is markedly richer in Ni and poorer in Cu, Zn, Ag, and Cd than the irregular exsolution pyrrhotite produced by breakdown of the *Iss*. Rare, pyrrhotite-free chalcopyrite in sample 90MC10 contains more Zn and Cd than that in the Medvezhy Creek vein ores. Its composition differs notably from that of the chalcopyrite host to the intergrowth, which appears to have a high Ni content, as well as relatively high Ga, Pd, and Ag contents. Within the chalcopyrite host to the intergrowth, measured Ni and Pd concentrations may be partly due to invisible, exsolved inclusions of pentlandite, as the Ni contents of 1 and 2.6 wt.% are high and erratic.

Based on the data of Smirnov (1966), sample 90MC10 is typical of sulfide-rich, picritic–taxitic gabbrodolerite. From several tens of analyses of borehole samples, Smirnov calculated average Cu/Ni ratios for various ore types in the Noril'sk I intrusion as follows: picritic gabbrodolerite, overall 1.29, high-grade 1.50; taxitic gabbrodolerite, overall 1.58, high-grade 1.74. Data from Table 1 can be used to calculate the composition of the sulfide component in sample 90MC10, and the data of Czamanske & Moore (1977) provide a basis for evaluation of the degree of evolution of this composition in terms of Cu/Ni ratio. By using a broad electron-microprobe beam and integration procedures, Czamanske & Moore determined bulk compositions for immiscible sulfide globules (11–223 μm across) in glassy, quenched rinds on samples of primitive and differentiated basalt from the Mid-Atlantic Ridge. The average composition (wt.%) for 13 globules in 11 samples of primitive olivine and picritic basalt is Fe 42.3, Ni 13.2, Cu 9.4, S 34.3, Cu/Ni 0.71; for 27 globules in 12 samples of plagioclase-bearing basalt, the average composition is Fe 49.1, Ni 6.9, Cu 9.2, S 33.9, Cu/Ni 1.34. Taking a value for S of 34.2 wt.%, and assuming that all of the Ni and Cu is sulfide-bound, the composition of the sulfide component in sample 90MC10 can be calculated as Fe 45.4 (by difference), Ni 7.7, Cu 12.7, S 34.2, Cu/Ni 1.65. Consideration of these Cu/Ni ratios indicates that the sulfide component of sample 90MC10 is far too evolved to be compatible with the relatively mafic rocks that host this ore type. Development of the physical, chemical, and isotopic attributes of this prevalent ore type in an upper-crustal environment is difficult to envision.

Pentlandite composition

Pentlandite in the Noril'sk–Talnakh ores varies widely in composition, particularly in Ni/Fe ratio and Co, Cu, and Pd contents. Shishkin *et al.* (1971), Distler *et al.* (1977), and Genkin *et al.* (1973, 1981) discussed the composition of Noril'sk–Talnakh pentlandite in some detail, mostly with reference to the significant differences in Ni/Fe ratio and Pd content that characterize distinct types of massive ore associated with the Kharaelakhsky and Talnakh intrusions.

Pentlandite forms as a result of subsolidus reactions at temperatures at or below 610°C (Craig & Kullerud 1969, Kullerud *et al.* 1969, Hill 1984) and changes composition as it continues to equilibrate to low temperatures. The Ni/Fe ratio in pentlandite is determined by the coexisting sulfide-mineral assemblage (which reflects the bulk composition of the ore) and temperature of equilibration; this compositional dependence of Ni/Fe ratio in pentlandite can also be expressed in terms of sulfur fugacity (Harris & Nickel 1972, Misra & Fleet 1973, Kaneda *et al.* 1986), as schematically shown by the equation,

$$9\mathrm{FeS} + (\mathrm{Fe}_{0.33}\mathrm{Ni}_{0.66})_9\mathrm{S}_8 = 2(\mathrm{Fe}_{0.66}\mathrm{Ni}_{0.33})_9\mathrm{S}_8 + 1/2\ \mathrm{S}_2.$$

The Ni/Fe ratios (atomic) of pentlandite in the samples studied are appropriate for the assemblages, as documented by Harris & Nickel (1972), who suggested that in most cases the composition of pentlandite indicates re-equilibration below 135°C. Over the range of Ni/Fe ratios from 0.66 to 1.78, the atomic metal:sulfur (M/S) ratio in pentlandite varies irregularly between 1.110 and 1.135, with the exception that the ratio is 1.097 in the exsolution pentlandite of sample 90KMZ5; a range of M/S ratios is typical of each of the ore types of Table 3. Ni/Fe ratios in pentlandite are lowest (0.66–0.82) in samples of cupriferous, pyrrhotite-free massive ore (combinations of mooihoekite, talnakhite, pentlandite, cubanite, and magnetite) from the Oktyabr'sky mine. Ni/Fe ratios in pentlandite vary from 0.84 to 1.00 in samples of massive sulfide from the Oktyabr'sky mine that contain the assemblage pyrrhotite – chalcopyrite – pentlandite – magnetite, and show a weak inverse correlation with the Cu content of these samples (4.02–22.5 wt.%). Pentlandite in Medvezhy Creek vein ore (assemblages dominated by chalcopyrite and cubanite) is characterized by significantly higher Ni/Fe ratios (1.06–1.13); these vein samples vary widely in bulk composition (11.6–28.0 wt.% Cu) and sulfide mineral proportions. These results are generally consistent with data presented by Genkin *et al.* (1973) and Distler *et al.* (1977). Pentlandite in samples 90OC1 and 90OC25 contains as much Ni (42.9, 44.5 wt.%, respectively) as any pentlandite analyzed by Harris & Nickel (1972); as one might anticipate from their report, the pentlandite containing 44.5 wt.% Ni is associated with godlevskite (plus bornite and chalcopyrite). Genkin *et al.* (1981) reported 44.6, 46.1, and 46.6 wt.% Ni in pentlandite in three samples of ore containing chalcopyrite and bornite, but we are not aware of any compositional data for pentlandite specified to be in association with godlevskite in the Noril'sk–Talnakh district.

Pentlandite containing 42.9 wt.% Ni occurs near the upper contact of the Kharaelakhsky orebody in disseminated chalcopyrite–pentlandite ore in contact gabbrodolerite (sample 90OC1). This pentlandite composition is of interest because it demonstrates that significant differences in Ni/Fe ratio in pentlandite occur in spatially associated samples. The gabbrodolerite is cut by chalcopyrite – pentlandite – magnetite veins (sample 90OC2) in which the Ni content of pentlandite is 33.7 wt.%, and sample 90OC1 was taken only a few tens of meters from massive talnakhite-bearing samples 90OC5 and 90OC14, in which the Ni contents of pentlandite are 30.5 and 28.4 wt.%, respectively. If one can safely extrapolate the experimental work of Kaneda *et al.* (1986) to low temperatures, the difference in sulfur fugacity corresponding to these compositional differences is about 10^4, with higher sulfur fugacity corresponding to greater Ni/Fe ratio. Genkin *et al.* (1981) reported that in the Noril'sk–Talnakh ores, it is not unusual to find that sulfide-mineral assemblages differ notably between adjacent matrix and droplet ores, or between a picritic gabbrodolerite host and leucogabbro inclusions within it. We believe that this juxtapostion of mineral assemblages and mineral compositions occurs because the ore-bearing intrusions are products not only of multiple intrusive events and complex patterns of re-equilibration, but of continued differential movement during the emplacement process.

Genkin *et al.* (1981) stated that the pentlandite associated with mooihoekite and talnakhite contains Cu. On the basis of the data of Shishkin *et al.* (1971), it might be more correct to have said that it typically contains more Cu than pentlandite in pyrrhotite-bearing ore. Our data support this conclusion, but measured Cu contents of large (1–2.5 cm across) porphyroblastic grains of pentlandite in Cu-rich ore are 0.12 to 0.41 wt.%, lower than the contents of 0.49 to 0.61 wt.% reported by Shishkin *et al.* Similar Cu contents characterize coarse porphyroblastic pentlandite (Pn_1) in association with chalcopyrite and cubanite in Cu-rich Medvezhy Creek vein ores.

There is poor correlation between the Ni and Co contents of analyzed pentlandite, and no overlap between the Co contents of pentlandite in samples of the three ore types of Table 3. Nickel contents of pentlandite range from 30.7 to 33.8 wt.% in massive pyrrhotite-bearing ores and from 26.9 to 30.5 wt.% in massive, pyrrhotite-free cupriferous ores of the Otyabr'sky mine, and from 34.7 to 36.0 wt.% in the Cu-rich Medvezhy Creek vein ores; respective Co contents are 1.01 to 1.88, 0.72 to 0.96, and 0.25 to 0.48 wt.%. Distinctly higher Co contents of pentlandite in pyrrhotite-bearing ore apparently reflect preference of Co for the *Mss* (resulting in higher bulk Co contents in ores enriched by settling of *Mss*), and subsequently for the pentlandite structure. For both pyrrhotite-bearing and pyrrhotite-free ores, there is a strong positive correlation between the Co content of pentlandite and the bulk Co/Ni ratio of the ore. Kaneda *et al.* (1986) suggested that the Co content of pentlandite exsolved from pyrrhotite correlates with the Co/Ni ratio of the high-temperature, homogeneous pyrrhotite. Co contents of pentlandite from our sample suite correlate strongly with bulk Co/Ni ratio, suggesting that the compositional control noted by Kaneda *et al.* (1986) extends to all varieties of pentlandite regardless of their ultimate derivation (see below). In ores from the Oktyabr'sky mine, there is a decrease in Ni/Fe ratio in pentlandite with increasing Cu content of the ore, apparently reflecting a concomitant decrease in sulfur fugacity (Kaneda *et al.* 1986).

Palladium concentrations in pentlandite do not correlate well with Ni/Fe ratio in pentlandite or with bulk Pd concentration in the sample. Based on knowledge of the Talnakh ores and experimental studies, Distler *et al.* (1977, their Figs. 4 and 6) suggested that Pd concentration in pentlandite is related both to its Ni/Fe ratio and to total Pd content in the ore. (Because our data on Pd concentration are not normally distributed, they were transformed into logarithms to allow proper testing of the significance of these correlations.) Figure 7A shows that for our suite of samples, the overall correlation between Pd concentration and Ni/Fe ratio in pentlandite is an artifact of mixed populations of samples. (The apparent trend for pyrrhotite-free Oktyabr'sky ores is meaningless, as Pd contents in these ores are at the MDL.) There is also no overall correlation between the bulk Pd content of the samples studied and Ni/Fe ratio in the contained pentlandite (Fig. 7B). Figures 7A and 7B do suggest that for the more rapidly quenched Medvezhy Creek vein ores, there is a good correlation between the bulk Pd content of the sample and Pd concentration in pentlandite; for these samples alone there is support for the contention of Distler *et al.* (1977, their Fig. 6) that correlations may exist between total Pd content of

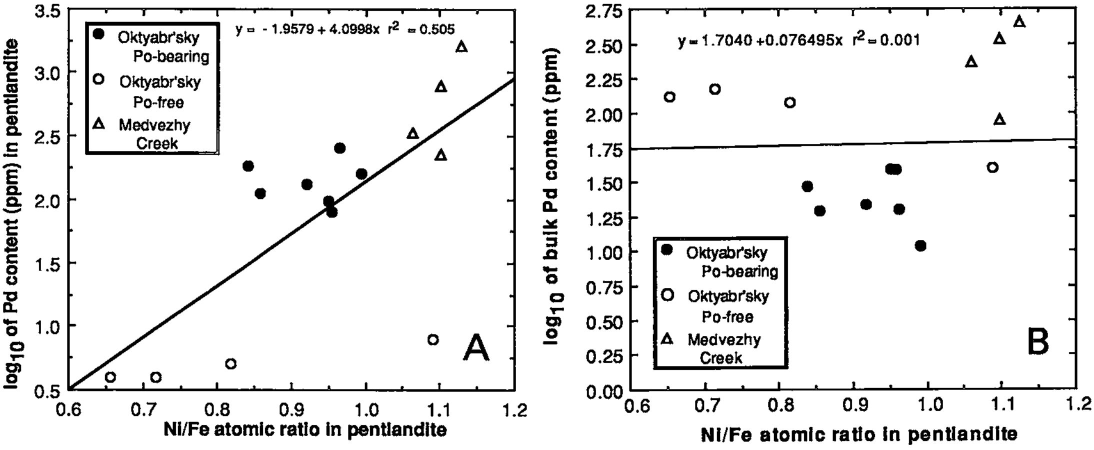

FIG. 7. Plots of Ni/Fe ratio in pentlandite against (A) its Pd content and (B) bulk Pd concentration in the sample.

the ore, Pd concentration in pentlandite, and Ni/Fe ratio in pentlandite.

We do not believe that Ni/Fe ratio in pentlandite commonly controls Pd concentration in pentlandite. Because the empirical observations of Harris & Nickel (1972) and the experimental studies of Kaneda *et al.* (1986) demonstrate than pentlandite composition (*i.e.*, Ni/Fe ratio) is a function of sulfur fugacity, we also maintain that sulfur fugacity, *per se*, does not control the solubility of Pd in pentlandite. We suggest that bulk composition and the sequence of crystallization from high-temperature sulfide liquids most directly control the amount of Pd ultimately held in solid solution in pentlandite.

Pentlandite petrogenesis

The range of Pd concentrations in pentlandite is significant (< 5–2540 ppm) within our sample suite, but comparable to concentrations measured by proton microprobe from other magmatic Cu–Ni sulfide deposits (Table 5). The diverse compositions and assemblages represented by the sample suite have allowed examination of causes for this variation and development of an explanation for it. Aside from three texturally unusual samples (90MC10, 90OC1, 90OC21), our suite of samples can be divided into four groups, only one of which is typically pyrrhotite-bearing. (1) Massive pyrrhotite – chalcopyrite – pentlandite ore; Pd concentrations in pentlandite range from 68 to 284 ppm. (2) Cu- and PGE-enriched massive ore from the Oktyabr'sky mine, in which pentlandite forms large, porphyroblastic crystals in intergrowths of chalcopyrite-group minerals; Pd concentrations in pentlandite range from < 5 to 8 ppm. (3) Cu- and PGE-enriched ore that forms veinlets or segregations in massive ore or adjacent country rock in upper parts of the Oktyabr'sky mine; pentlandite forms large, porphyroblastic grains and contains from < 5 to 14 ppm. (4) Cu- and PGE-enriched sulfide veins that cut picritic gabbrodolerite in the Medvezhy Creek open pit; pentlandite forms large porphyroblastic grains or chains of grains at the margins of large grains of chalcopyrite and contains from 203 to 2540 ppm Pd. In order to focus comparison of these ore types, bulk compositional data are summarized in Table 6 for samples that are comparable in Cu content. As implied by this table, contents of Fe, Ni, S, Co, and Zn are considered no more important to the issue than Cu content. Other elements have been listed either because some role in this issue has been ascribed to them (As, Sn, Sb, Te, Pb, Bi) or to emphasize how dramatically their concentrations vary in the three ore types (Se, Ag, Cd, Au, Pd, Pt). Silver, Cd, Sn, Sb, Bi, and especially Pb are far more enriched in the Cu-rich ores of the Oktyabr'sky

TABLE 5. RANGES OF Pd CONTENTS (ppm) OF PENTLANDITE DETERMINED BY PROTON MICROPROBE FOR MAGMATIC ORES FROM THE NORIL'SK–TALNAKH AND OTHER DEPOSITS

Noril'sk			
Medvezhy Creek mine			
disseminated ore	(1,5)*	po-cpy-pn-cb; droplets in picritic-taxitic gabbrodolerite (see text for description of textures in sample 90MC10)	237 to 710
massive vein ore	(4,17)*	cupriferous assemblages (cpy-pn with variable proportions of cb; po in one sample); pn occurs as large, porphyroblastic grains or chains of grains	203 to 2,540
Talnakh			
Oktyabr'sky mine			
disseminated ore	(1,4)*	cpy-pn	all analyses below MDL
massive ore	(7,26)*	po-cpy-pn±cb; pn forms relatively small grains (<5 mm) texturally associated with po	68 to 284
	(3,10)*	cupriferous assemblages (mh, tk, cb, pn); pn occurs as large, porphyroblastic grains	<5 to 8
massive vein ore	(3,10)*	cpy-pn with variable proportions of bn, cb, ga, po, and gd; pn occurs as large, porphyroblastic grains	<5 to 14
	(1,4)*	cpy-ga-pn-cb; pn forms small grains (<1 mm)	8 to 402
Komsomolsky mine			
massive ore	(1,9)*	po-cpy-pn-py; pn in exsolution and replacement textures	127 to 254
Sudbury	(25)+	mill concentrate	<1.2 to <3
Stillwater, J-M Reef	(10)++	pn texturally associated with po	1,870 to 13,650
Bushveld	(43)+++	assemblages unknown	<10 to 980

* This study, where (x,y) indicates the number of samples, x, and the number of analyses, y.

\+ Cabri *et al.* (1984; 25 analyses).

++ Cabri *et al.* (1984; 10 analyses).

+++ Paktunc *et al.* (1990; 41 analyses); Cabri (1988; 2 analyses).

TABLE 6. BULK TRACE–ELEMENT COMPARISON OF Cu–RICH ORES WITH DISSIMILAR CONTENTS OF Pd IN PENTLANDITE

	OKTYABR'SKY			MEDVEZHY CREEK
	Massive ore		Vein ore	Vein ore
	Po-bearing*	Po-free	Po-free	Po-free
Cu, wt.%	20.5-22.5	28.2-29.0	26.4	24.3-28.0
As, ppm	0.24-0.55	1.2-6.6	8.1	2.2-10
Se	90-110	120-209	93	218-328
Ag	30-37	130-270	90	26-73
Cd	10-17	43-52	20	<6-15
Sn	8.5-20	40-85	15.8	9.6-25
Sb	<0.05-0.52	1.4-2.9	1.4	0.25-1.2
Te	8-16	28-80	14	57-210
Au	1.5-1.9	2.2-5.3	5.5	1.2-11
Pb	100-230	600-790	240	<10-10
Bi	1.7-4.9	8.2-13	7.2	3.8-7.8
Pd	29-39	77-149	40	233-445
Pt	3.0-7.5	20-26	34	39-215
Pn (Ni/Fe)+	0.84-0.95	0.66-0.72	1.09	1.06-1.13

Data summarized from Table 1 and Appendix I.

* Samples represented from Oktyabr'sky: massive po-bearing, 90OC13, 90OC29, 90OMZS1-3; massive po-free, 90OC9, 90OC14, 90OMZS1-1; vein ore 90OC2; from Medvezhy Creek 90MC15, 90MCZC1, 90MC5.

\+ Range of Ni/Fe (atomic) in pentlandite.

mine, whereas Se, Te, Pd, and Pt are more enriched in the Cu-rich Medvezhy Creek vein ores.

In massive ore samples that contain the assemblage pyrrhotite – chalcopyrite – pentlandite, the pentlandite forms small grains (< 5 mm across) along the margins of large pyrrhotite grains or occurs as thin lamellae in pyrrhotite. Bulk compositions of these samples fall within the solid-solution field of *Mss* at high temperature, as determined by experimental studies in the Fe–Ni–S and Cu–Fe–Ni–S systems (Kullerud *et al.* 1969, Craig & Kullerud 1969, Hill 1984), and these ores probably solidified between 850° and 800°C. Consistent with textures in these ores, we conclude that pentlandite formed by exsolution from *Mss* below 610°C. Makovicky *et al.* (1986) experimentally demonstrated that the solubilities of Pd, Pt, Ru, and Rh in pyrrhotite decrease sharply between 900°C and 500°C, depending on bulk composition. With decreasing temperature, Pd will be rejected from the high-temperature pyrrhotite structure and probably enters pentlandite, which can hold at least twenty times as much Pd, Rh, and Ru as coexisting pyrrhotite at 500°C (Makovicky *et al.* 1986). The Pd content of pentlandite in this assemblage will depend upon the Pd content of the *Mss* at the time of pentlandite formation, the distribution coefficient between the two phases, and possible low-temperature migration of Pd to inter- or intragranular PGM (*e.g.*, Makovicky *et al.* 1988, their Fig. 5 and our Medvezhy Creek vein samples). In turn, the Pd content of the *Mss* will have been determined by the Pd content of the sulfide liquid and the distribution coefficient between sulfide liquid and *Mss*, as well as possible diffusion of Pd from *Mss* prior to pentlandite exsolution.

In Cu-rich massive ores such those of the Kharaelakhsky orebody or that occur as veins in the Oktyabr'sky or Medvezhy Creek mines, pentlandite must have had a different origin. In these ores, pentlandite typically forms large (1–2.5 cm), subhedral porphyroblastic grains that are associated with chalcopyrite-group minerals; pyrrhotite is absent. Bulk compositions of these ores typically fall within or near intermediate-temperature, solid-solution limits of the *Iss*, which expand significantly down to about 600°C (*e.g.*, Cabri 1973) to encompass the bulk compositions of the mooihoekite- and talnakhite-rich massive ores. Experimental studies of the Cu–Fe–S and Cu–Fe–Ni–S systems (Kullerud *et al.* 1969, Craig & Kullerud 1969, Dutrizac 1976, Hill 1984) provide some constraints on crystallization sequences. However, despite these and numerous other experimental studies, one can outline only generally the intermediate and end stages of crystallization from the chemically complex Noril'sk–Talnakh ores. Bulk compositions corresponding to the Cu-rich ores may begin to crystallize *Mss* on the liquidus below 1000°C and will crystallize *Iss* on the liquidus at about 900°C (Dutrizac 1976). Tie lines may be established between *Iss* and *Mss*, and a quaternary Cu–Fe–Ni–S liquid may coexist with *Mss* and *Iss* at 850°C (Craig & Kullerud 1969, their Fig. 3). Segregations of this more S-rich, late fractionate may be represented by samples 839, 90OC21, and 90OC25, in which mooihoekite and talnakhite are absent. According to Kullerud *et al.* (1969), liquid fields disappear in the ternary systems at 813°C (Cu–Fe–S), 635°C (Fe–Ni–S), and 572°C (Cu–Ni–S). It is not at all straightforward to predict solidus temperatures for the Cu-rich ore compositions at Noril'sk–Talnakh (*cf.* Makovicky *et al.* 1988); it is likely that the ores were largely solid at 800°C, but that small amounts of liquid persisted to quite a low temperature, partly owing to concentration of trace elements. Craig & Kullerud (1969) noted that *Iss* coexisting with *Mss* may contain as much as 15 wt.% Ni at 600°C; pentlandite was not found in their experiments. However, Hill (1984) noted the presence of pentlandite in his investigations of part of the Cu–Fe–Ni–S system at 600°C; where bulk compositions produced the pentlandite–*Mss*–*Iss* assemblage, the *Iss* was found to contain 1.4 to 2.63 wt.% Ni. Bulk Ni contents of 2.5, 2.6, 3.5, and 3.8 wt.% characterize the mooihoekite- and talnakhite-rich massive ores of the Kharaelahksky orebody, whereas 6.0, 6.5, and 7.1 wt.% Ni are found in the three Cu-rich Medvezhy Creek vein samples of Table 6 (data for sample 90MC16 are not included here or in Table 6, as geochemical and mineralogical characteristics show that this sample is distinct from, and possibly transitional into, the Cu-rich ore represented by the other three Medvezhy Creek vein samples); both ore types may represent *Iss* compositions constrained in different ways.

We believe that in the Cu-rich ores, pentlandite formed large, porphyroblastic grains by exsolution from Ni-bearing *Iss*, which eventually unmixed to form chalcopyrite-group minerals. We suggest the possibility that only ores that now contain pyrrhotite ever contained *Mss* in excess of that which was later absorbed by *Iss*; in other words, all pyrrhotite-free ores may be products of liquid fractionation in which the Fe content was low enough to be entirely consumed in formation of pentlandite and chalcopyrite-group minerals. This proposal is in keeping with the Fe-poor composition of pentlandite in the pyrrhotite-free ores. It raises the further intriguing possibility that the crystallization of pentlandite may drive the associated Cu–Fe–S phases toward, or away from, mooihoekite and talnakhite compositions, depending on the bulk composition of the *Iss*. This would be comparable to the effect of pentlandite crystallization from *Mss*, which is to leave the remainder of the system more S-rich. Finally, we cannot preclude the possibility that pentlandite may have been able to crystallize directly from the Cu-rich ores. Clearly, the Noril'sk–Talnakh ores merit a comprehensive, state-of-the-art experimental study of crystallization sequences and low-temperature phase relations in the Cu–Fe–Ni–S system!

As shown in Table 5, the Pd concentrations in pentlandite in Cu- and PGE-enriched ores lie at the extremes of the measured range of concentration. Pentlandite from the Cu-rich veins at Medvezhy Creek contains 203 to 2540 ppm Pd, as compared to Pd concentrations of <5 to 14 ppm for pentlandite in Cu-rich massive ores and veins from the Oktyabr'sky mine. Bulk compositions and sulfide-mineral assemblages differ only slightly, and Pd concentrations are only 2 to 3 times higher for the Medvezhy Creek vein ores; these differences are too slight to account for the several orders of magnitude difference in the Pd concentrations in pentlandite in pyrrhotite-free ore from the two mines.

A detailed study of PGM paragenesis has not been made for our samples, but observations with the SEM suggest that PGM formed over a wide range of temperatures and that different sequences of crystallization may characterize different types of ore. The timing of PGM crystallization is a controversial subject, with emphasis commonly placed on extremes, rather than acknowledging that PGM form over a broad temperature range in response to diverse conditions. Certain PGM may crystallize directly from sulfide liquids at high temperatures and subsequently undergo phase transformations and reactions at lower temperatures; other PGM likely form by exsolution from high-temperature sulfide phases (Makovicky *et al.* 1986); whereas yet other PGM are only stable at low temperatures, are associated with low-temperature mineral phases enriched in incompatible or volatile components, and occur in veins or show other textural evidence for late crystallization. Makovicky *et al.* (1990) suggested that (Pd,Pt)S containing from 5 to 13.1 at.% Ni may have formed at temperatures ranging from 900°C down to 470°C. Distler *et al.* (1977) noted that the paragenesis of the Pt–Pd minerals changes with sulfur activity. They, as well as Genkin *et al.* (1973), Razin *et al.* (1973), and Genkin & Evstigneeva (1986), established that in the Talnakh deposit Pd occurs principally in solid solution in pentlandite in pyrrhotite-bearing ores; as Pd-sulfide minerals (*e.g.*, cooperite, braggite, vysotskite) in chalcopyrite-rich, veinlet, and breccia ores; and as intermetallic compounds with Te, Bi, and Sb in talnakhite-bearing ores.

We suggest that two processes may be responsible for the minimal Pd concentrations typical of pentlandite in the Cu-rich massive ores of the Kharaelakhsky orebody and, further, that relatively rapid crystallization of the Cu-rich Medvezhy Creek vein ores may have inhibited both of these processes; (1) Pd-bearing PGM may have crystallized from *Iss* as early high-temperature phases, and (2) Pd may have preferentially accumulated with other trace elements in residual low-temperature liquids. The Pd content of pentlandite derived by crystallization from *Iss* should be controlled by the concentration of Pd in the *Iss* and the distribution coefficient of Pd between *Iss* and pentlandite. Makovicky *et al.* (1986) concluded that Pt, Pd, Rh, and Ru are generally insoluble in *Iss* because concentrations of Pt, Rh, and Ru in *Iss* at 500°C and 900°C and of Pd in *Iss* at 500°C were found to be below their electron-microprobe detection limit of ~500 ppm. As this level of concentration is well above the bulk concentration of Pd in Noril'sk–Talnakh ores, significant solubility of Pd in *Iss* cannot be precluded. If Pd-bearing PGM formed prior to crystallization of pentlandite in the massive, Cu-rich Kharaelakhsky ores, Pd concentrations in the *Iss* may have been several orders of magnitude lower when pentlandite crystallized in those ores than when it crystallized in the Cu-rich vein ores at Medvezhy Creek.

There is evidence for high-temperature PGM crystallization in the massive Cu-rich ores of the Kharaelakhsky orebody. Some intergrowths of Pd–Sn minerals observed in samples of this ore obviously formed by exsolution from a primary Pd–Pt–Sn phase; this primary phase had an idiomorphic habit and now occurs as isolated grains, or associated with skeletal magnetite in chalcopyrite-group minerals. Our cursory observations of PGM (Appendix I) indicate a distinction between the two Cu-rich ores; Pd- and Pt-bearing, Sn and Bi minerals predominate in the Oktyabr'sky mine samples, and Pd- and Pt-bearing alloys, arsenides, tellurides, and bismuthotellurides predominate in Medvezhy Creek vein samples. Razin *et al.* (1973), Genkin *et al.* (1981), and Genkin & Evstigneeva (1986) noted that coarse-grained Sn- and Pb-bearing Pt and Pd minerals are common in massive Cu-rich ore. These minerals, which often exhibit euhedral and skeletal forms and occur as inclusions in Cu–Fe–Ni sulfide minerals, are termed "metacrystals" (*i.e.*, porphyroblasts) by Genkin & Evstigneeva, but the textures also are compatible with high-temperature crystallization. Platinum-group minerals that are binary compounds of Pd with Sn or Pb commonly have melting points of more than 1000°C (Berlincourt *et al.* 1981), which may allow crystallization of these minerals at temperatures well above the stability limit of pentlandite, even in chemically complex systems.

On the other hand, there is ample reason to believe that a low-melting liquid, enriched in trace elements, may have been present well below temperatures of *Iss* solidification and pentlandite exsolution. Multiphase aggregates of PGM in the Cu-rich Oktyabr'sky ores typically occur at grain boundaries and are commonly measured in fractions of a millimeter. Within these aggregates, textural relations among three or four combinations of coexisting Pd, Pt, Bi, and Sn minerals, as well as such phases as PbTe and electrum, suggest late-stage crystallization. The data of Table 6 substantiate enrichment of trace, intermetallic elements in the pyrrhotite-free ores that one would expect in a low-melting, late-stage Cu-rich liquid; if these trace elements preferentially resided in dispersed droplets of liquid in solidified *Iss*, their concentrations within the droplets would have been much higher. By the time pentlandite became stable below 610°C, it is probable that there existed dispersed droplets of liquid enriched in critical trace elements, such that Pd preferentially entered the droplets (to ultimately form a variety of PGM), rather than the pentlandite structure. As the annealing time for the ore mass must have been protracted, the observations of Genkin & Evstigneeva (1986) regarding sequences of transformation of early to later PGM suggest that if Pd entered pentlandite at a high temperature, it may have diffused and migrated to enrich PGM aggregates during cooling.

Genkin & Evstigneeva (1986) believed that in the Noril'sk–Talnakh ores Pt, Pd, Sn, Te, Pb, As, Sb, and Bi were concentrated initially into a Cu-rich liquid and subsequently into a low-melting, residual liquid that was dispersed among crystalline sulfides. They based this conclusion on a number of observations: (1) in mooihoekite- and talnakhite-bearing ores, PGM are most generally found in interstices between grains and along microfissures, not uncommonly associated with a volatile-enriched phase, such as the Cl-bearing sulfide mineral djerfisherite; (2) the relatively large PGM in these sites almost invariably form complex polymineralic aggregates, which may have variable bulk composition, even where in close proximity; (3) large, skeletal PGM are interpreted to be "metacrystals" and contain inclusions of pyrrhotite, chalcopyrite, cubanite, and talnakhite; (4) PGM are often concentrated in pockets along the upper contacts of massive orebodies; and (5) veinlets containing euhedral PGM crystals cut base-metal sulfides.

Several studies suggest that some intermetallic, Pd-bearing PGM cannot have formed early; Hoffman & MacLean (1976) showed that michenerite (PdBiTe; one of the most common PGM in the our samples of the Cu-rich veins at Medvezhy Creek) melts at about 500°C, Skinner *et al.* (1976) found that the liquid in the Fe–Pd–S system becomes increasingly Pd-rich until it crystallizes at 570°C, and Makovicky *et al.* (1990) reported that inadvertent addition of Ni to this system lowered the field of stability of the melt to at least 500°C. Berlincourt *et al.* (1981) summarized experimental studies, which show that many of the intermetallic, Pd-bearing PGM, particularly those containing As, Bi, and Te, have low melting points, consistent with low-temperature crystallization. Because of the common occurrence of polymineralic aggregates in the Sudbury ores and the low melting or breakdown temperatures of many PGM, Cabri & Laflamme (1976) suggested that PGE were concentrated in dispersed droplets of residual liquid in *Iss*. They noted that the crystallization of chalcopyrite from *Iss* at ~550°C may liberate PGE to form PGM.

We believe that the Cu-rich Medvezhy Creek vein ores were emplaced as high-temperature sulfide liquids of comparable origin to the Cu-rich liquid of the Kharaelakhsky orebody, and may be regarded as complementary to the massive pyrrhotite veins that predominate in the lower parts of the Noril'sk I intrusion. We suggest that Pd concentrations in pentlandite in the pyrrhotite-free, Cu-rich veins at Medvezhy Creek are several orders of magnitude higher than Pd concentrations in pentlandite in pyrrhotite-free ores from the Oktyabr'sky mine because more rapid quenching did not permit either a prolonged early period of PGM crystallization or segregation of droplets of low-melting residual liquid. Significantly lower concentrations of Ag, Bi, Cd, Sb, Sn, and, especially, Pb (Table 6) may have had a role in inhibiting these processes during crystallization of these veins. PGM in our samples of Cu-rich Medvezhy Creek vein ore typically measure only a few μm across and occur within Cu–Fe–Ni sulfide grains, commonly pentlandite. [Note that this mode of occurence is not typical of all ore types of the Noril'sk I intrusion, as Genkin (1959) described ores containing PGM >1 mm across.] These PGM are most commonly monomineralic, but not uncommonly two-phase (*e.g.*, $PtAs_2 + PdNiAs$ or $PtAs_2 + PdBiTe$). With the exception of one irregular, large (150 × 200 μm) grain of Pt-Fe alloy in sample 90MCZC1, PGM in these PGE-rich ores commonly measure less than 5 μm across. Thus, some Pd locally combined with critical trace elements within sulfide mineral grains, but high concentrations of Pd were left in solid solution in the pentlandite structure. The distribution of PGM in pentlandite, though less dense, nonetheless is thought to reflect the type of exsolution process illustrated by Makovicky *et al.* (1988, their Fig. 5).

It is possible that the primary sulfide liquid associated with the Medvezhy Creek ores differed in composition from that of the Kharaelakhsky orebody. However, the relatively modest enrichment of the Cu-rich Medvezhy Creek vein ores in the suite of most volatile trace elements (Table 6) is precisely what might be predicted for early separation of a Cu-rich liquid from an *Mss*-rich assemblage. We propose that elemental migration upward through the cumulus pile of *Mss* and interstitial liquid in the Kharaelakhsky orebody may have further enriched that large pool of Cu-rich sulfide liquid in Ag, Cd, Sn, Sb, Bi, and Pb. On a grand scale, comparable to observations based on the droplet ore of sample 90MC10, one can envision that this less dense, Cu-rich liquid fraction accumulated in the upper, central part of the crystallizing sulfide mass and remained relatively isolated between the solidified intrusion above and a largely crystalline mass of *Mss* and interstitial sulfide liquid below. Between the liquidus and solidus temperatures of this entire Kharaelakhsky ore mass, there would have been a protracted period of time during which preferential migration of trace elements into the Cu-rich liquid could take place by diffusion. We also suggest that during this interval of crystallization, the S-deficient character of the abundant mooihoekite–talnakhite ores and the unusual presence of troilite in ores of intermediate "stratigraphic" position (Figs. 3, 4) developed as a result of extended crystallization of *Mss* (a relatively S-rich phase) and possible loss of S to the overlying intrusion if H_2 was available for formation of H_2S.

Selenium and sulfur

In the dominant Cu–Fe–Ni sulfide minerals of the Noril'sk–Talnakh district, Se is more uniformly distributed among the coexisting phases than S. The data of Kovalenker *et al.* (1974) suggest this to be the case and show, as do our data, that Se is enriched in the upper part of the Kharaelakhsky orebody. Paktunc *et al.* (1990) concluded from their study of other Cu–Ni sulfide occurrences that Bi, Se, and Te are equally abundant in pyrrhotite, chalcopyrite, and pentlandite. Bismuth concentrations are below the MDL in the samples we analyzed, and the distribution of Te is relatively uniform among coexisting sulfide minerals. For massive ore, Se concentrations in coexisting sulfide phases are remarkably uniform; statistical coefficients of variation for Se concentrations range from 0.023 to 0.198, with six values less than 0.05. (The single value of 10 ppm for pyrrhotite in sample 90OC12 was excluded.) The data are presented in the box and whisker plot of Figure 8. This result is so compelling as to cause one to search for explanations in cases were Se concentrations in coexisting phases are not comparable, *e.g.*, the atypically low Se content of lamellar cubanite in sample 839. Our ranges of Se concentrations in chalcopyrite, pyrrhotite, and pentlandite are compared to proton-microprobe data for other well-known Cu–Ni sulfide deposits in Figure 9. (Note that although the ranges for Noril'sk–Talnakh are comparable to one another, they might be even

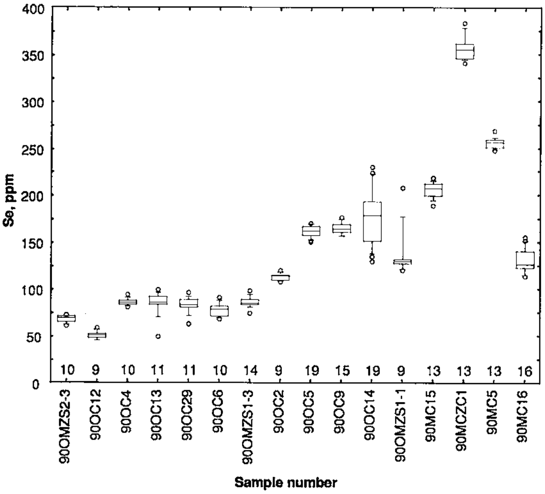

FIG. 8. Box and whisker diagram for Se concentrations in all Cu–Fe–Ni sulfide minerals in a given sample. Top of box represents 75th percentile, bottom of box 25th percentile; top tick represents 90th percentile, bottom tick 10th percentile. Median is line through box; circles represent values below and above 10th and 90th percentiles, respectively. Total number of analyses for each sample shown inside figure.

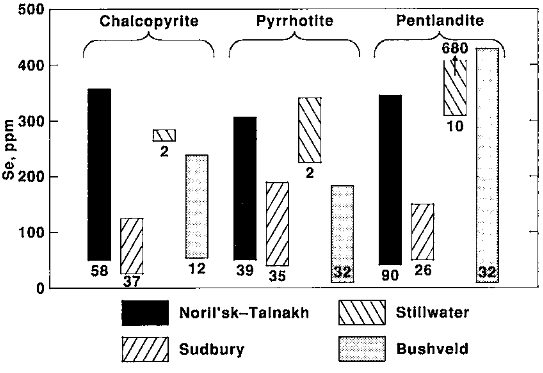

FIG. 9. Total ranges of Se concentration in chalcopyrite, pyrrhotite, and pentlandite from the Noril'sk–Talnakh district, compared to comparable proton-microprobe data for other well-known Cu–Ni–PGE deposits. Number of analyses represented by each bar is indicated.

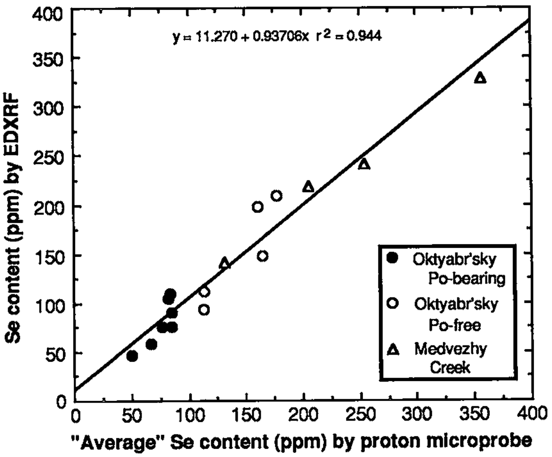

FIG. 10. Comparison of "average" (see text) Se concentrations for each sample as determined by proton microprobe, with bulk Se concentrations determined by high-precision EDXRF.

more similar, but for the fact that some samples lack one or another mineral.) Selenium concentrations obtained by duplicate EDXRF analyses of bulk ore powders are compared in Figure 10 with concentrations obtained by simply averaging all proton-microprobe determinations for Se in a given sample. Considering the fact that this averaging procedure takes no account of the modal proportions of minerals, the result is another indication of the uniformity of Se distribution among the minerals. Also clearly indicated in Figure 10 is the fact that virtually all of the Se in the ores is carried in the major sulfide minerals.

Cabri *et al.* (1984) noted that despite ambiquities that cloud early promise that Se/S ratios can resolve contributions of magmatic and sedimentary S, the accuracy of Se determinations for individual minerals by proton microprobe renews interest in this genetic and geochemical problem. Paktunc *et al.* (1990, their Table 6) summarized much of the available data for Se/S ratios in the dominant minerals of Cu–Fe–Ni sulfide deposits and noted that the mantle range for $(\mathrm{Se/S}) \times 10^6$ is 230-350. Bulk weight ratios of $(\mathrm{Se/S}) \times 10^6$ for our samples range from 130 to 990 (mean 330; average 390). These relatively high Se/S ratios appear to exclude local derivation of S from Permian anhydrite, as a sample of marly Permian anhydrite in association with ore was analyzed and found to contain <5 ppm Se. The overall Se/S ratios that characterize the ores (Kovalenker *et al.* 1974 and this study) would require an anomalously high magmatic value of $(\mathrm{Se/S}) \times 10^6$ if 30–40% of the S contained in the ores was derived from a source that had a Se/S ratio similar to that of the analyzed anhydrite. Based on Se/S ratios, crustal assimilation of S cannot have been an important process unless it involved an unproven, Se-enriched source such as black shale.

An important and controversial aspect of the ores of the Noril'sk–Talnakh district is that their S-isotopic compositions are heavier than would be expected for uncontaminated magmatic Cu–Ni sulfide deposits. However, S-isotopic compositions are quite uniform for individual ore-bearing intrusions. For ores associated with the Noril'sk and Talnakh intrusions, $\delta^{34}\mathrm{S}$ averages about 9.3‰, whereas in the Kharaelakhsky orebody of the Kharaelakhsky intrusion, $\delta^{34}\mathrm{S}$ averages about 11.6‰ (Kovalenker *et al.* 1974). Kovalenker *et al.* have established that these distinctions in isotopic composition are valid for all Cu–Fe–Ni sulfide minerals in the Talnakh and Kharaelakhsky ores. As the Talnakh orebody lies above the Kharaelakhsky orebody (40–400 m *versus* 400–1,500 m depth), these authors proposed that the difference in average S-isotopic composition between the two deposits relates to preferential upward mobility of $^{32}\mathrm{S}$. To account for the relatively uniform and heavy values of $\delta^{34}\mathrm{S}$ that characterize ores of the Noril'sk–Talnakh district, Kovalenker *et al.* (1974), Gorbachev & Grinenko (1973), and numerous other authors have called upon assimilation of as much as 30–40% of isotopically heavy, crustal sulfur, with subsequent homogenization with mantle-derived sulfur in an intermediate chamber. Grinenko (1984), perhaps accepting the problems attendant on bulk assimilation of material containing such a large quantity of sulfur, later proposed that the mafic magmas were sulfurized by gases rich in hydrogen sulfide and, presumably, of heavy S-isotopic composition. With either of these models, lifting of sulfide liquid remains a problem, as the homogeneous isotopic composition of sulfur in the ores would seem to require that sulfur was added to the magmas in a staging chamber well beneath the level of emplacement of the ore-bearing intrusions. As noted earlier, the metal concentrations associated with the Noril'sk–Talnakh intrusions pose a problem perhaps even more difficult to explain than the isotopically heavy sulfur that characterizes the ores. On the basis of many considerations, including study of the Pb-isotopic compositions of the ores (Wooden *et al.* 1991, Czamanske *et al.* 1992), we too believe that staging chambers played an important role in the evolution of the Noril'sk–Talnakh deposits, and envision that they served primarily as reservoirs in which immiscible sulfide liquid of mantle derivation was concentrated from enormous volumes of basaltic liquid, prior to emplacement with the special class of fully differentiated, ore-bearing intrusions.

Kyser (1990), in a recent review of data relating to variation in stable isotope composition in the lithospheric mantle, concluded that all stable isotope ratios are more variable in the continental lithospheric mantle than in the modern oceanic mantle. This seems to be especially true for S, for which the commonly perceived, limited range typical of the mantle, 0 ± 2‰ is actually only characteristic of the modern oceanic mantle; a number of spinel peridotites have been analyzed for which $\delta^{34}S$ ranges from 4 to 25‰ (*e.g.*, Chaussidon *et al.* 1987, Kyser 1990). Eldridge *et al.* (1991) used the ion microprobe to determine that $\delta^{34}S$ ranges from 8 to 14‰ in sulfide inclusions in diamond from Sierra Leone. We believe that the uniformly heavy $\delta^{34}S$ in the Noril'sk–Talnakh ores reflects an extreme of mantle heterogeneity, relating either to unhomogenized primordial accretion and early convection or to subduction of crustal material; the heterogeneity may have been lithospheric or asthenospheric.

ACKNOWLEDGEMENTS

G.K. Czamanske gratefully acknowledges that this work is the culmination of an interest in detailed ore petrology engendered over 20 years ago under the stimulating tutelage of Paul Barton. The support of J.L. Campbell and W.J. Teesdale at the University of Guelph was enthusiastic. Robert Hershiser provided superb polished surfaces, and J.H.G. Laflamme and P. Carrière gave technical assistance. Evgenii Sereda not only introduced us to the complexities of Noril'sk mineralogy, but shared important samples from his collection. We acknowledge the reviews of Jim Craig and Larry Hulbert and the substantial improvements to the manuscript that were forced by the incisive comments of Paul Barton.

REFERENCES

BASALTIC VOLCANISM STUDY PROJECT (1981): *Basaltic Volcanism on the Terrestrial Planets.* Pergamon Press, New York.

BERLINCOURT, L.E., HUMMEL, H.H. & SKINNER, B.J. (1981): Phases and phase relations of the platinum-group elements. *In* Platinum-Group Elements: Mineralogy, Geology, Recovery (L.J. Cabri, ed.). *Can. Inst. Mining Metall., Spec. Vol.* **23**, 19-45.

BETHKE, P.M. & BARTON, P.B., JR. (1971): Distribution of some minor elements between coexisting sulfide minerals. *Econ. Geol.* **66**, 140-163.

CABRI, L.J. (1973): New data on phase relations in the Cu–Fe–S system. *Econ. Geol.* **68**, 443-454.

______ (1988): Applications of proton and nuclear microprobes in ore deposit mineralogy and metallurgy. *Nucl. Instr. Meth. Phys. Res.* **B30**, 459-465.

______, BLANK, H., EL GORESY, A., LAFLAMME, J.H.G., NOBILING, R., SIZGORIC, M.B. & TRAXEL, K. (1984): Quantitative trace-element analyses of sulfides from Sudbury and Stillwater by proton microprobe. *Can. Mineral.* **22**, 521-542.

______, CAMPBELL, J.L., LAFLAMME, J.H.G., LEIGH, R.G., MAXWELL, J.A. & SCOTT, J.D. (1985): Proton-microprobe analysis of trace elements in sulfides from some massive-sulfide deposits. *Can. Mineral.* **23**, 133-148.

______ & LAFLAMME, J.H.G. (1976): The mineralogy of the platinum-group elements from some copper-nickel deposits of the Sudbury area, Ontario. *Econ. Geol.* **71**, 1159-1195.

CAMPBELL, J.L. & COOKSON, J.A. (1984): PIXE analysis of thick targets. *Nucl. Instr. Meth. Phys. Res.* **B3**, 185-197.

______, MAXWELL, J.A., TEESDALE, W.J., WANG, J.-X. & CABRI, L.J. (1990): Micro-PIXE as a complement to electron probe microanalysis in mineralogy. *Nucl. Instr. Meth. Phys. Res.* **B44**, 347-356.

CHAUSSIDON, M., ALBARÈDE, F. & SHEPPARD, S.M.F. (1987): Sulfur isotope heterogeneity in the mantle from ion microprobe measurements of sulfide inclusions in diamonds. *Nature* **330,** 242-244.

CLAOUÉ-LONG, J.C., ZHANG, ZICHAO, MA, GUOGAN & DU, SHAOHUA (1991): The age of the Permian–Triassic boundary. *Earth Planet. Sci. Lett.* **105,** 182-190.

COOMBES, J.S. (1991): *Platinum 1991.* Johnson Matthey Public Ltd. Co., London.

CRAIG, J.R. & KULLERUD, G. (1969): Phase relations in the Cu–Fe–Ni–S system and their application to magmatic ore deposits. *In* Magmatic Ore Deposits (H.D.B. Wilson, ed.). *Econ. Geol., Monogr.* **4**, 344-358.

______, NALDRETT, A.J. & KULLERUD, G. (1968): Succession of mineral assemblages in pyrrhotite-rich Ni-Cu ores. *Carnegie Inst. Wash. Year Book* **66**, 431-434.

CZAMANSKE, G.K. & MOORE, J.G. (1977): Composition and phase chemistry of sulfide globules in basalt from the Mid-Atlantic Ridge rift valley near 37°N. lat. *Geol. Soc. Am. Bull.* **88**, 587-599.

______, WOODEN, J.L., BOUSE, R.M., ZIENTEK, M.L., LIKHACHEV, A.P., KUNILOV, V.E. & LYUL'KO, V. (1992): Pb isotopic data indicate a complex, mantle origin for the Noril'sk–Talnakh ores, Siberia. *Econ. Geol.* **87**, in press.

DALRYMPLE, G.B., CZAMANSKE, G.K., LANPHERE, M.A., STEPANOV, V. & FEDORENKO, V.A. (1991): ^{40}Ar/^{39}Ar ages of samples from the Noril'sk–Talnakh ore-bearing intrusions and the Siberian flood basalts, Siberia. *Eos (Am. Geophys. Union Trans.)* **72**, 570 (abstr.).

DEYOUNG, J.H., SUTPHIN, D.M., WERNER, A.B.T. & FOOSE, M.P. (1985): International strategic minerals inventory summary report - nickel. *U.S. Geol. Surv., Circ.* **930-D**.

DISTLER, V.V., CHIRINA, N.A. & BELOUSOV, G. YE. (1974): Rhodium in pyrrhotite from copper–nickel ore of the Noril'sk deposits. *Dokl. Acad. Sci. USSR, Earth Sci. Sect.* **214**, 205-208.

______, MALEVSKIY, A. YU. & LAPUTINA, I.P. (1977): Distribution of platinoids between pyrrhotite and pentlandite in crystallization of a sulfide melt. *Geokhimiya* (11), 1646-1657 [also *Geochem. Int.* **14**(6), 30-40].

DUTRIZAC, J.E. (1976): Reactions in cubanite and chalcopyrite. *Can. Mineral.* **14**, 172-181.

DYUZHIKOV, O.A., DISTLER, V.V. & STRUNIN, B.M. (1988): *Geology and Ore Deposits of the Noril'sk District.* Nauka, Moscow (in Russ.).

ELDRIDGE, C.S., COMPSTON, W., WILLIAMS, I.S., HARRIS, J.W. & BRISTOW, J.W. (1991): Isotopic evidence for the involvement of recycled sediments in diamond formation. *Nature* **353**, 649-653.

FEDORENKO, V.A. (1981): Petrochemical series of extrusive rocks of the Noril'sk region. *Geologiya i Geofizika* (6), 78-88 [also *Sov. Geol. Geophys.* **22**(6), 66-74].

______ & DYUZHIKOV, O.A. (1981): Hyperbasite–basite effusive volcanism of the Noril'sk region. *Sovetskaya Geologiya* (9), 98-106 (in Russ.).

______, STIFFEEVA, G.T., MAKEEVA, L.V., SUKHAREVA, M.S. & KUZNETSOVA, N.P. (1984): Basic and alkali-basic intrusions of the Noril'sk region in connection with their comagmatism with effusive formations. *Geologiya i Geofizika* (6), 56-65 [also *Sov. Geol. Geophys.* **25**(6), 54-61].

GENKIN, A.D. (1959): Conditions of occurrence and characteristics of the composition of platinum group minerals in ores of the Noril'sk deposit. *Geol. Rudnykh Mestorozhdenii* **1**(6), 74-84 (in Russ.).

______, DISTLER, V.V., GLADYSHEV, G.D., FILIMONOVA, A.A., EVSTIGNEEVA, T.L., KOVALENKER, V.H., LAPUTINA, I.P., SMIRNOV, A.V. & GROKHOVSKAYA, T.L. (1981): *Sulfide Copper–Nickel Ores of the Noril'sk Deposits.* Nauka, Moscow (in Russ.).

______, ______, LAPUTINA, I.P. & FILIMONOVA, A.A. (1973): Geochemistry of palladium in copper-nickel ores. *Geokhimiya* (9), 1336-1343 [also *Geochem. Int.* **10**, 1007-1013].

______ & EVSTIGNEEVA, T.L. (1986): Associations of platinum-group minerals of the Noril'sk copper–nickel sulfide ores. *Econ. Geol.* **81**, 1203-1212.

______ & VYAL'SOV, L.N. (1967): Valleriite and mackinawite and conditions of their occurrence in ores. *Geol. Rudnykh Mestorozhdenii* **9**(2), 94-106 (in Russ.).

GORBACHEV, N.S. & GRINENKO, L.N. (1973): Origin of the Oktyabr'sky sulfide-ore deposit, Noril'sk region, in the light of sulfide and sulfate sulfur isotope compositions. *Geokhimiya* (8), 1127-1136 [also *Geochem. Int.* **10**, 843-851].

GREZ, E., AGUILAR, A., HENRIQUEZ, F. & NYSTROM, J.O. (1991): Magnetita Pedernales: a new magmatic iron deposit in northern Chile. *Econ. Geol.* **86**, 1346-1349.

GRINENKO, L.N. (1984): Hydrogen sulfide-containing gas deposits as a source of sulfur for sulfurization of magma in ore-bearing intrusives of the Noril'sk area. *Dokl. Akad. Nauk SSSR* **278**, 730-732 [also *Int. Geol. Rev.* **27**, 290-292].

HARRIS, D.C., CABRI, L.J. & NOBILING, R. (1984): Silver-bearing chalcopyrite, a principal source of silver in the Izok Lake massive-sulfide deposit: confirmation by electron- and proton-microprobe analyses. *Can. Mineral.* **22**, 493-498.

______ & NICKEL, E.H. (1972): Pentlandite compositions and associations in some mineral deposits. *Can. Mineral.* **11**, 861-878.

HILL, R.E.T. (1984): Experimental study of phase relations at 600°C in a portion of the Fe–Ni–Cu–S system and its application to natural sulphide assemblages. *In* Sulphide Deposits in Mafic and Ultramafic Rocks (D.L. Buchanan & M.J. Jones, eds.). Institute of Mining and Metallurgy, London (14-21).

HOFFMAN, E. & MACLEAN, W.H. (1976): Phase relations of michenerite and merenskyite in the Pd–Bi–Te system. *Econ. Geol.* **71**, 1461-1468.

KANEDA, H., TAKENOUCHI, S. & SHOJI, T. (1986): Stability of pentlandite in the Fe–Ni–Co–S system. *Miner. Deposita* **21**, 169-180.

KARPENKOV, A.M., RUDASHEVSKY, N.S. & SHUMSKAYA, N.I. (1981): The natural chloride of palladium and bismuth - the phase of $Pd_4Bi_5C_{13}$ composition. *Zap. Vses. Mineral. Obshchest.* **110**, 86-91 (in Russ.).

KOVALENKER, V.A., GLADYSHEV, G.D. & NOSIK, L.P. (1974): Isotopic composition of sulfide sulfur from deposits of the Talnakh ore mode in relation to their selenium content. *Int. Geol. Rev.* **17**, 725-734.

______, LAPUTINA, I.P., YEVSTIGNEYEVA, T.L. & IZOITKO, V.M. (1976): Thalcusite, $Cu_{3-x}Tl_2Fe_{1+x}S_4$, a new thallium sulfide from copper–nickel ores of the Talnakh deposit. *Int. Geol. Rev.* **19**, 108-112.

KULAGOV, E.A., EVSTIGNEEVA, T.L. & YUSHKO-ZAKHAROVA, O.E. (1969): Godlevskite (a new iron-nickel sulfide). *Geol. Rudnykh Mestorozhdenii* **11**(3), 115-121 (in Russ.).

KULLERUD, G., YUND, R.A. & MOH, G.H. (1969): Phase relations in the Cu–Fe–S, Cu–Ni–S, and Fe–Ni–S systems. *In* Magmatic Ore Deposits (H.D.B. Wilson, ed.). *Econ. Geol., Monogr.* **4**, 323-343.

KYSER, T.K. (1990): Stable isotopes in the continental lithospheric mantle. *In* Continental Mantle (M.A. Menzies, ed.). Clarendon Press, Oxford, U.K. (127-156).

MAKARENKO, G.F. (1976): The epoch of Triassic trap magmatism in Siberia. *Int. Geol. Rev.* **19**, 1089-1100.

MAKOVICKY, E., KARUP-MØLLER, S., MAKOVICKY, M. & ROSE-HANSEN, J. (1990): Experimental studies in the phase systems Fe–Ni–Pd–S and Fe–Pt–Pd–As–S applied to PGE deposits. *Mineral. Petrol.* **42**, 307-319.

MAKOVICKY, M., MAKOVICKY, E. & ROSE-HANSEN, J. (1986): Experimental studies on the solubility and distribution of platinum group elements in base-metal sulphides in platinum deposits. *In* Metallogeny of Basic and Ultrabasic Rocks (M.J. Gallagher, R.A. Ixer, C.R. Neary & H.M. Prichard, eds.). The Institute of Mining and Metallurgy, London (415-425).

______, ______ & ______ (1988): Experimental evidence on the formation and mineralogy of platinum and palladium ore deposits. *In* Mineral Deposits Within the European Community (J. Boissonnas & P. Omenetto, eds.). Springer, Berlin (303-317).

MAXWELL, J.A., CAMPBELL, J.L. & TEESDALE, W.J. (1989): The Guelph PIXE software package. *Nucl. Instr. Meth. Phys. Res.* **B43**, 218-230.

MILANOVSKIY, YE.YE. (1976): Rift zones of the geologic past and their associated formations. Report 2. *Int. Geol. Rev.* **18**, 619-639.

MISRA, K.C. & FLEET, M.E. (1973): The chemical composition of synthetic and natural pentlandite assemblages. *Econ. Geol.* **68**, 518-539.

NALDRETT, A.J. (1969): A portion of the system Fe–S–O between 900 and 1080°C and its application to sulfide ore magmas. *J. Petrol.* **10**, 171-201.

PAKTUNC, A.D., HULBERT, L.J. & HARRIS, D.C. (1990): Partitioning of the platinum-group and other trace elements in sulfides from the Bushveld Complex and Canadian occurrences of nickel–copper sulfides. *Can. Mineral.* **28**, 475-488.

RAZIN, L.V., BEGIZOV, V.D. & MESHCHANKINA, V.I. (1973): Data on mineralogy of platinum metals in the Talnakh deposit. *Int. Geol. Rev.* **17**, 6-56.

SHISHKIN, N.N., MITENKOV, G.A., MIKHAYLOVA, V.A. & KARPENKOV, A.M. (1971): Pentlandite from massive ore of the Talnakh and Oktyabr'skoye deposits in the Talnakh ore zone. *Dokl. Acad. Sci. USSR, Earth Sci. Sect.* **197**, 112-115.

______, ______, ______, RUDASHEVSKIY, N.S. & SIDEROV, A.F. (1974): Nickel, cobalt, and copper in pyrrhotite from massive ores of the Talnakh ore cluster. *Geokhimiya* (1), 95-104 (also *Geochem. Int.* **11**, 76-84).

SKINNER, B.J., LUCE, F.D., DILL, J.A., ELLIS, D.E., HAGAN, H.A., LEWIS, D.M., ODELL, D.A., SVERJENSKY, D.A. & WILLIAMS, N. (1976): Phase relations in ternary portions of the system Pt–Pd–Fe–As–S. *Econ. Geol.* **71**, 1469-1475.

SMIRNOV, M.F. (1966): *The Structure of Noril'sk Nickel-Bearing Intrusions and the Genetic Types of Their Sulfide Ores.* Nedra, Moscow (in Russ.).

VAUGHAN, D.J. & CRAIG, J.R. (1978): *Mineral Chemistry of Metal Sulfides.* Cambridge University Press, New York.

WOODEN, J.L., CZAMANSKE, G.K. & BOUSE, R.M. (1991): Pb isotopic constraints on the origin of the Cu–Ni–PGE ores of the Noril'sk–Talnakh district, Siberia. *EOS, Am. Geophys. Union Trans.* **72**, 571 (abstr.).

ZONENSHAIN, L.P., KUZMIN, M.I. & NATAPOV, L.M. (1990): Geology of the USSR: A Plate-Tectonic Synthesis. *Am. Geophys. Union, Geodynamics Ser.* **21**.

Received August 20, 1991, revised manuscript accepted December 1, 1991.

APPENDIX I. PROTON- AND ELECTRON-MICROPROBE DATA FOR MAJOR NI-FE-CU SULFIDE MINERALS (PPM, EXCEPT WT.% FOR FIGURES WITH DECIMALS).

	Co*	Ni*	Cu	Zn	Ga	Se	Pd	Ag	Cd	In	Sn	Te	Pb
90OMZS2-3 (po-cpy-pn)													
Pn (4,1.00,1.124)**	1.32	33.8	130,85,<79	--***	--	64,68,69	159,159,152	--	--	15,<10,9?	15,<8,<10	--	--
Po (6,0.915,0.30)	0.02	3010,3130 3030,2960	--	--	--	69,71,72 71	--	<6,<6,11 8	--	--	--	--	--
Cpy	n.d.+	<240	X++	435,396,202	<34,<34,40	64,63,61	--	7,6?,8	<9,10<8	<9,11,<9	17,18,<10	<17,<16,30	--
90OC12 (po-cpy-pn)													
Pn (4,0.97,1.135)	1.54	33.1	72?,<73,108 137	--	--	45,48,45 47	224,284,281 229	--	--	--	--	--	<21,<21,<21 70
Po (4,0.923,0.20)	0.13	2210,2090 1730	<33,74,167	--	--	53,50,10	--	--	--	8?,<7,<7	--	--	--
Cpy	n.d.	<225	X	211,237,272	40?,<36,52	50,52,59	<6,<6,6?	<7,7?,<6	<8,9?,10	--	13,<12,<10	--	79,295,164
90OC4 (cpy-po-pn)													
Pn (5,0.92,1.116)	1.10	32.5	117,<74,<73 <76	--	--	94,85,83 80	119,106,165 132	16,10,6? 6?	--	<9,<10,12 8?	--	--	(Sb-13,23)+++
Po (3,0.907,0.15) (3,0.983,0.00)	0.11 0.12	1530,1660 1530	73,<33,56	--	--	88,87,86	--	--	--	--	17,<9,9	--	--
Cpy	n.d.	<224	X	260,174,476	<35,33?,36	88,83,82	--	--	9,15,15	--	<11,10?,<11	--	42,<23,<23
90OC13 (cpy-po-pn)													
Pn (4,0.95,1.130)	1.86	32.5	<77,136,<75 <78, 188	--	--	82,87,95 84,79	68,92,80 81,*313*	<6,<6,<6 10,<6	--	--	11,<9,<9 <9,*122*	<16,12,<16 <17,21	<22,<22,<22 67,<22
Po (8,0.913,0.21) (4,0.988,0.09)	0.03 0.03	1570,1330 1720	52,39,<33	--	--	90,82,49	--	--	--	--	--	<13,19,<14	--
Cpy	n.d.	<220	X	233,269,197	<35,40,41	83,87,99	<6,6?,<6	10,8,9	9,11,9	--	14,10,<9	<19,16?,15?	63,78,<22
90OC29 (cpy-po-pn)													
Pn (2,0.95,1.134)	1.88	32.3	--	--	--	87,83,81 77,63	83,106,135 88,68	--	--	--		--	380,<21,80 114,37
Po (5,0.913,0.22) (4,0.980,0.04)	0.01 0.02	1720,1570 2120	54,<33,<33	--	--	86,89,80	--	--	--	--		--	(Ru-17,21, 14)
Cpy	n.d.	<225	X	558,261,468	37?,33?,31?	89,79,96	--	--	17,6?,6?	--	14,16,17	17?,18,<18	250,137,166
90OC6 (po-cpy-pn)													
Pn (3,0.86,1.132)	1.01	31.4	--	<42,<45,53	--	68,70,70	119,93,115	<6,81,10	--	--	--	--	<21,40,<21
Po (4,0.913,0.10) (4,1.003,0.08)	0.13 0.12	1250,1070 330,817	<33,71,<33 129	--	--	84,77,80 81	<5,6,4.6? <5	7,<6,4.5? 5?	--	--	--	--	--
Cpy	n.d.	<225	X	246,169,107	--	79,91,74	--	--	9,15,11	--	--	--	267,148,39

	Co	Ni	Cu	Zn	Ga	Se	Pd	Ag	Cd	In	Sn	Te	Pb
90OMZS1-3 (cpy-po-cb-pn)													
Pn (3,0.84,1.122)	1.27	30.7	--	--	--	82,85,84	177,182,182	14,11,7	--	13,<10,<10	--	16,<14,<14	<22,95,<21
Po (4,0.960,0.07)	0.02	645,740 306	<14,19,16	--	--	88,85,74	--	--	8,<7,<6	--	--	--	(Ru-4.1?<4,4.5) (Rh-5.8,4?,3.2?)
Cpy	n.d.	<217	X	186,246	34?,<33	88,81	--	--	14,15	--	--	--	(As-8?,9)
Cb	n.d.	<180,***672***	X	171,188,253 117,107,***636***	<31,42,<32 50,45,<32	85,98,92 89,93,81	<6,<5,<5 <5,28,<6	6?,<6,11 7,10,<6	<8,<7,8? <6,9,***26***	(As-12,13 10,<16<10 <8)	14,<10,<10 15,16,9?	<17,35,<15 <15,17,<15	<23,178,71 114,196,81
90OC2 (cpy-pn)													
Pn (4,1.09,1.114)	0.98	33.7	948,1250 479,117 443,335	--	--	109,115,112 115,108,109	<6,<6,<6 14,14,***243***	4?,13,20 10,11,22	11,<7,6? 6?,<7,6?	--	<11,<11,<11 <11,<11,***117***	26,<16,27 <17,<15,23	146,156,344 686,565,167
Cpy	n.d.	<224	X	140,81,79	<38,38?,39?	120,114,114	<6,7,<6	11,17,53	14,10,23	9?,18,12	<12,18,<12	18,30,<20	339,596,306
90OC5 (mh-cb-pn)													
Pn (7,0.82,1.115)	0.80	30.5	91,383,129 503,123	<45,67,<44 51,44?	--	151,150,155 157,157	<5,<6,<6 ***26,62***	39,16,<7 8,15	--	--	<11,8?,<7 ***18,32***	29,75,50 67,55	132,133,137 454,182
$\mathrm{Cb_M}$	n.d.	299,<189 209,315	X	<48,94,156 ***630***	44,41,<36 <36	164,170,162 170	6,15,27 14	9,<7,<6 22	11,11,<8 ***67***	<9,<9,20 <9	<10,<11,15 15	59,64,36 72	349,105,162 407
$\mathrm{Cb_L}$	n.d.	193?,244 2465,193? 339	X	366,186,340 153,431	35?,47,<34 32?,42	161,162,169 168,159	<6,6.5,7 ***15,142***	31,24,15 41,32	22,10,21 22,16	<9,16,<9 <9,<9	<11,<11,<11 ***38,67***	84,61,51 60,55	110,123,92 80,139
Mh (Sb-12,16)	n.d.	1900,2000 2100,2300 2300	X	62,<52,<54 114,103	45,38,<35 51,53	163,155,168 161,163	<6,<6,7? <7,***25***	<7,6?,53 42,22	8?,8?,<7 10, 9	11,13,11 13,20	13,<11,12 <12,***16***	91,38,64 74,93	145,72,60 69,151
90OC9 (mh-cb-pn)													
Pn (6,0.66, 1.122)	0.96	26.9	332,357,262 363	--	--	168,164,159 159	--	<7,<7,8 6	--	--	--	62,52,<20 46	--
$\mathrm{Cb_M}$	n.d.	<187,336 <180,299	X	<49,176<46 102	--	174,157,170 177	--	--	--	--	<9,<9,16 ***157***	47,23,57 52	47,66,54 52
$\mathrm{Cb_L}$	n.d.	3600,9800 16700	X	77,<48,68	--	163,166,165	--	58,102,155	12,20,27	--	33,27,17	33,54,28	56,43,34
Mh	n.d.	4650,4600 5400,4250	35.8	74,<52,<52 <52	42,49,43 <35	157,163,161 171	--	26,<6,14 <6	--	12,14,14 <9	28,14,16 15	30,43,52 38	<25,63,38 41

	Co	Ni	Cu	Zn	Ga	Se	Pd	Ag	Cd	In	Sn	Te	Pb
90OC14 (tk-cb-pn)													
Pn (5,0.72,1.119)	0.72	28.4	4060,100 430,372	--	--	143,150,150 135	<5,<6,<5 ***14***	6?,14,12 ***62***	8?,5?,5? <7	--	--	77,73,93 69	<23,104,<21 61
Cb$_M$	n.d.	<177,<175 207,<176 <177,<177	X	<47,<46<47 ***144,433*** ***1840***	<32,<33,<33 34,44,<34	193,165,153 129,186,188	<5,<5,<6 <5,<9,***61***	43,<6,<6 <6,<10,10	13,10?,10 ***27,62,220***	--	<11,<9,<10 <9,<18,***52***	17?,54,71 31,72,43	164,75,155 65,67,168
Cb$_L$	n.d.	527,<228 <174,<179	X	94,125,184 <46	40,30?,38 <32	224,230,219 163	--	49,45,50 57	108,31,18 10	--	19,15?,30 25	84,95,81 96	121,78,90 44
Tk	n.d.	6100,5600 4400,3550 3800,5850	35.7	<54,80,84 59,<53,115	<36,<36,38 <38,<36,42	218,192,177 189,156,208	<8,<8,<8 <8,<8,***38***	45,13,42 65,10,17	<10,<11,12 11,<8,<10	<12,10?,<12 11,15,17	29,33,<18 <13,<12,***55***	128,85,91 111,85,94	50,54,<31 <24,66,62
90OMZS1-1 (tk-mh-cb-pn)													
Cb$_M$	n.d.	<183,<186	X	--	<32,45	132,130	--	--	--	--	<11,18	18,38	--
Cb$_L$	n.d.	443,520	X	73,***231***	<34,37	122,130	--	15,17	<8,***39***	(Sb-14,25)	14,22	25,34	38,<23
Tk	n.d.	9600,9500	36.6	--	36,32?	120,131	--	27,<7	10,8?	9?,<9	--	<21,18?	--
Mh	n.d.	5900,6350	35.1	--	52,<34	128,128	9,3.6?	13,8	8?,<8	<9,14	--	(Sb-26,15)	<23,39
90OC1 (cpy-pn)													
Pn (4,1.78,1.112)	1.16	42.9	322,321 <83,1310	--	--	103,108,103 113	--	10,33,7? <7	--	--	--	34,35,29 <10	590,1340 <22,3170
Cpy	n.d.	337,250 311,370	X	80,91,***526*** ***1730***	40?,<35,45 35?	112,116,113 116	30,12,96 34	11,11,18 12	<8,11,***13*** ***68***	15,11,<10 <10	25,19,16? 43	--	223,221,202 158
90KMZ5 (po-cpy-pn)													
Pn$_R$ (4,1.26,1.111)	1.11	37.3	450,506,420 200,400,480	--	--	71,71,81 83,79,80	234,230,196 127,189,254	--	--	--	--	(Rh-<4,7, <5,<5,<5, 10)	(Pt-<33, <35,83,<37, <37,103)
Pn$_E$ (3,1.22,1.097)	1.18	36.1	<76,<77 1360	<42,83,<46	--	86,80,84	210,134,170	26,30,26	--	14,<9,11	--	--	--
Po (2,0.858,0.82)	0.07	7870,7680 7910,10460	99,360,68 <36	--	--	86,71,88 90	--	--	--	--	--	16,<12,<13 <13	--
Py	n.d.	430,197	<12,135	--	--	55,78	--	--	--	--	--	22,<12	--

	Co	Ni	Cu	Zn	Ga	Se	Pd	Ag	Cd	In	Sn	Te	Pb
90MC10 (po-cpy-pn-cb)													
Pn (2,0.98,1.119)	0.82	33.6	<77,<75,110 <77,<77	--	--	117,113,140 106,111	237,386,263 525,710	46,12,14 17,9	--	<11,<12,<11 16,<11	(Ru-5,14, <5,7,7)	10?,19,<16 <14,24	(Rh-28,27 <5,21,17)
Po$_{M}$ (2,0.883,0.26)	0.07	2350,2170 2930	42,36,<18	--	--	152,149,112	4?,11,<4.6	--	<7,<7,8?	--	--	12?,<16,12?	(Rh-12,12, 11)
Po$_{I}$ (3,0.859,0.08)	0.06	704,630 654,814	565,837 3080,422	1240,234 897,1234	--	128,152,149 112	<4.5,<4.7,6 6	16,55,63 10	20,<7,23 27	--	--	<14,34,29 <14	--
Cpy$_{M}$	n.d.	726,<210	X	796,616	--	100,96	--	8,11	12,20	--	<11,13	37,31	29?,33
Cpy$_{I}$	n.d.	10280,26100	X	847,527	44,47	127,113	19,35	69,40	12,9?	--	--	--	54,38?
Cb	n.d.	985	X	178	--	147	7	20	--	--	11	--	--
90MC16 (cpy-cb-po-pn)													
Pn (2,1.10,1.122)	0.63	35.7	1430,5457	--	--	114,121	203,249	21,23	--	--	<10,8.6?	16,<10	--
Po (3,0.879,0.07)	0.11	539,717,755	25,17,86	--	--	126,124,132	--	--	--	--	--	15,<13,<12	(Rh-4.6,4.9, <4.2)
Cpy	n.d.	329,1118 <215,2750 4305	X	66,<51,49? 109,64	55,<33,44 42,61	140,146,126 140,135	<6,<6,<6 19,<6	13,19,54 54,25	<7,8,9 13,11	8?13,<9 <9,<9	--	38,37,<15 <18,24	--
Cb$_{M}$	n.d.	308,436	X	<46,88	<32,36	117,124	--	58,39	8?,9?	--	--	--	--
Cb$_{L}$	n.d.	<174,630 5240,456	X	92,62,***609*** ***1310***	36,<33,<33 <31	156,152,122 114	<5,<6,9 <5	86,92,62 58	12,<8,***21*** ***35***	<9,<9,11 7?	<10,19,<10 11	27,50,<14 <14	--
90MC15 (cpy-cb-pn)													
Pn (6,1.10,1.134)	4x 0.44 2x 0.25	35.7	600,230,145 <77	--	--	189,198,200 199	203,1033 811,1082	12,40,16 55	--	--	--	44,40,40 64	--
Cpy	n.d.	<225	X	80,125,54	43,<35,47	196,210,204	3?,7,5?	18,8,38	12,<9,<8	13,<9,11	<11,<10,12	38,53,61	--
Cb$_{L}$	n.d.	576,260,240	X	342,286,81	40,<33,<33	213,207,211	13,<6,<6	13,64,75	20,12,9	8?,<9,10	--	83,68,32	--
Mk (3,1.000)	0.46	8.16	1837,441 <69	--	--	209,218,215	556,400,476	49,22,38	<7,<7,6?	--	--	41,61,32	27,<21,29
90MCZC1 (cpy-cb-pn)													
Pn (4,1.06,1.110)	0.48	34.7	106,112,102	<46,<46,68	--	345,340,345	315,370,329	<7,8,59	--	13,16,<12	--	380,312,255	<22,36,<22
Cpy	n.d.	<228	X	<54,87,95	<35,38?,<34	351,344,356	25,32,19	108,91,105	--	<10,17,<10	--	329,360,274	--
Cb$_{L}$	n.d.	307,<188 263	X	114,278,137	--	355,354,362	50,32,11	141,159,128	<8,8?,9	11,9,7?	--	344,360,353	--
Mk (8,0.987)	0.50	7.63	916,110 1170,68	--	--	360,361,383 377	536,432,310 404	17,13,8 18	9,<7,<7 10	<12,16,<12 <12	--	384,301,341 384	88,<22,<23 <22

	Co	Ni	Cu	Zn	Ga	Se	Pd	Ag	Cd	In	Sn	Te	Pb
90MC5 (cpy-pn)													
Pn (7,1.13,1.120)	0.39	36.0	316,243,179 321,<77,724 <77,433	--	--	252,255,259 249,247,268 250,260	897,1170 1310,1350 1560,1860 2340,2540	40,16,12 55,8,42 <6,112	12,16,<8 <8,<8,<9 <8, <9	<16,<21,<20 28,22?,<24 <27,23?	--	61,86,83 117,63,81 84,54	<22,<23,28 70,<22,34 <23,<22
Cpy	n.d.	<220	X	--	--	257,258,249	8,21,12	17,23,19	<8,8?,9	--	--	143,80,82	--
Mk (2,0.985)	0.42	8.40	<70,190	<43,57	--	259,256	2150,2920	71,206	<9,11	<25,<30	10,14	67,80	<22,41
839 (cpy-pn-po-ga-cb)													
Pn (3,0.85,1.113)	0.69	31.1	--	--	--	247,254	--	18,11	8,<7	(Tl-128,44)	--	69,78	181,35
Po (3,0.909,0.08)	0.01	0.08	243,193	--	--	311,285	5?,<5	367,222	6?,<6	(Tl-<18)	22,33	228,158	799,596
Cpy	n.d.	414,403	X	333,286	39?,48	261,248	5?,<6	118,119	23,18	(Tl-45,<26)	308,431	138,126	37,28
Cb	n.d.	<190	X	343,375	<33,54	18,32	--	16,17	7?,21	(Tl-<25,<27)	231,124	<15,34	<23,93
90OC21 (cpy-ga-pn-cb)													
Pn (4,0.91,1.122)	0.72	32.2	130,344,211 127	<45,120,<45 69	<45,66,<37 <42	53,38,38 39	8,52,185 402	16,47,211 189	<7,9,7? <8	(Tl-<25,796, 44,128)	<11,143,132 261	13?,151,64 131	51,371,167 331
Cpy	n.d.	<222	X	190,272,207	66,97,35?	47,67,54	22,<6,<6	28,29,21	25,20,16	(Tl-<25,43, 27)	11?,125,14	125,79,129	324,456,300
Cb_L	n.d.	<182,<187	X	--	<37,44	66,86	52,49	25,32	10,<7	(Tl-<28)	20,37	84,90	542,880
Mk (7,0.990)	0.73	6.69	3613,491 573	<42,<40,51	--	51,51,43	77,115,7	984,539,643	--	(Tl-105,135, 235)	205,141,72	95,125,124	1008,508 483
90OC25 (bn-cpy-pn-gd)													
Pn (8,2.11,1.122)	2.64	44.5	487,880,372	--	--	110,110,110	3.2?,<6,6	5.8?,<6,<6	--	--	--	15?,<13,<13	--
Cpy	n.d.	351,306	X	<53,135	<35,43	119,109	18,23	9,9	--	15,13	15,11	23,39	<23,58
Bn	n.d.	<360	X	<91	<56	75	19	65	<11	16	<17	26	<41
Gd (2,1.142)	0.46	64.3	944,1164 1746	<50,70,49?	<35	105,105,100	19,<6,<6	11,<6,8	<8	13,<9,<9	10?,<10,<10	<16	<24

Only a few analytical data-sets, shown by follow-up SEM studies to have been perturbed by an unnoticed inclusion, have been deleted from this compilation. Bold italic type has been used to highlight cases where simultaneous high values for commonly associated trace elements (e.g., Zn + Cd or Pd + Sn) lead one to assume the presence of an occult submicroscopic inclusion. Minimum detection levels (MDL) in the major sulfide minerals are listed in Table 4. The GUPIX program used at Guelph (Maxwell et al. 1989) provides an objective assessment of the presence of an element by indicating "Y", "N", or "?". If "?" appears, a value is estimated for the concentration of the element, even if that value is below the indicated MDL. Such values, when well below the nominal MDL, have not been reported here, but values just below or at the MDL are those followed by "?" in this appendix.

For each individual mineral (row), values for the concentration of each element are listed in strict sequence. Thus, any user may check for interelement relations or may fully recreate the complete trace-element analysis of a given point. *Values including decimals are in wt.% from electron-microprobe determinations. **First value is number of electron-microprobe analyses; second value is Ni/Fe (atomic) for pn or M/S (atomic) for po, mk, and gd. Third value for pn is M/S and for po is the electron-microprobe value for Ni (wt.%). For this study, pyrrhotite type has been based on M/S from the electron-microprobe data: monoclinic, 0.858–0.883; hexagonal, 0.907–0.923; and troilite, 0.980–1.003. The value 0.960 reported for sample 90OMZS1-3 represents finely unmixed troilite + hexagonal pyrrhotite. ***--, all determinations below MDL; "<" with value in body of table indicates specific MDL. $^{+}$n.d., high MDL by proton microprobe and not sought by electron microprobe. $^{++}$X, major, virtually invariant component. $^{+++}$additional trace-element; listed in random column in lieu of element at concentration less than MDL.

APPENDIX II
SAMPLE LOCATIONS AND DESCRIPTIONS

90OMZS2-3: Oktyabr'sky mine, Shaft 2; massive po–cpy–pn–mt ore. Cpy occurs as thin lenses in po and as clear areas as much as 4 mm across. Pn is present as selvages (commonly 0.5–1 mm wide) along cpy–po contacts. Po shows broad twin lamellae (as Fe and Co contents of contrasting bands are uniform). Abundant mt grains average 0.5 mm across. Also identified: ZnS.

90OC12: Oktyabr'sky mine, Shaft 2; massive po–cpy–pn–mt ore. Irregular areas of po (from 2 × 2 mm to 2 × 4 cm) are surrounded by cpy (2–8 mm wide). Pn occurs along cpy–po contacts. Amoeboid mt grains may be 1.5 mm long. Also identified: $PtAs_2$, PbS.

90OC4: Oktyabr'sky mine, Bend 59, Part 2; collected 1.5 m above the lower contact of the Kharaelakhsky orebody; massive cpy–po–pn–mt ore. Areas of unmixed po are highly irregular (as large as 4 × 8 mm); associated areas of pn reach 3 × 4 mm. Mt is sparsely present as grains averaging 1 mm^2. Also identified: PtBiTe, (PdPt)BiTe, PdBi, Pd_2Sn, AgTe, PbSe, PbS.

90OC13: Oktyabr'sky mine, Shaft 2; massive cpy–po–pn–mt ore. Areas of unmixed po show extremely irregular boundaries with cpy, and po occurs as a myriad of tiny wisps and irregular, crystallographically controlled lamellae in cpy. Patches of pn may reach 3 mm across, and mt grains, 1 mm. Also identified ZnS, PbS.

90OC29: Oktyabr'sky mine, Shaft 2; massive cpy–po–pn–mt ore. Cpy shows twin lamellae more than 6 × 22 mm. Rather regular areas of un mixed po range from 1 to 4 mm across, pn grains to 3 mm, and mt grains to 1 mm. Also identified: $PtAs_2$, PbS.

90OC6: Oktyabr'sky mine, Bend 59, Part 2; collected at lower contact of Kharaelakhsky orebody. Cpy-rich layer (1–1.2 cm thick) against footwall (90OC6A) is in sharp contact with po-rich ore above (90OC6B). Irregular wisps of po in the cpy-rich band resemble those in 90OC13. Areas of cpy in the po-rich ore are more free of inclusions. Areas of pn interstitial to cpy and unmixed po may reach 5 mm across, and mt grains, 1.5 mm. No trace phases seen.

90OMZS1-3: Oktyabr'sky mine, Shaft 1; massive cpy–po–cb–pn–mt ore. Mt and pn (as much as 2 mm across) are preferentially associated with irregular masses of po (as large as 4 × 8 mm). Mt grains may be long and thin (0.5 × 2 mm) and commonly appear to contour po masses. Cb lamellae are rather poorly defined in cpy, and more massive cb is associated with po. Also identified: Pt_2PdSn, (Pt,Pd)Sn, $(Pd,Pt)_2Sn$, PbS.

90OC2: Oktyabr'sky mine, Bend 67, Part 3; sample prepared from 4-6-cm-wide cpy–pn–mt vein cutting gabbrodolerite in Kharaelakhsky orebody. Vein contacts are irregular and gradational over 2 mm. Pn grains may be twinned, and as large as 0.8 × 2.5 cm; they are fractured and traversed (replaced?) by cpy veinlets from 0.01 to 0.1 mm wide. Cuneiform mt (<0.5 m across) occurs in pn and in relatively inclusion-free cpy. Also identified: Pd_2Sn, Ag.

90OC5: Oktyabr'sky mine, Bend 67, Part 5; collected near upper contact of the Kharaelakhsky orebody; massive mh–cb–pn–mt ore. Mh hosts pn grains as large as 1.2 × 1.8 cm and cb exsolution lamellae larger than 2 × 15 mm. Sparse resorbed mt grains may be 2 mm across. Also identified: $PtAs_2$, PdBi, Pd_2Sn, electrum, Ag, PbTe, PbS, valleriite.

90OC9: Oktyabr'sky mine; Shaft 1; massive mh–cb–pn ore. Mh hosts fractured pn grains as large as 1 × 1.7 cm and shows twin lamellae from 0.5 to 3 mm wide and more than 2.5 cm long. Massive cb irregularly surrounds pn and thin (0.2–0.5 mm) cb lamellae cut mh. Mt (<1 mm across) is sparse. Also identified: Pd_2Sn, (Zn,Cd)S, PbS, valleriite.

90OC14: Oktyabr'sky mine, Bend 67, Part 5; collected near upper contact of the Oktyabr'sky orebody; massive tk–cb–pn–mt ore. Mh hosts pn grains as large as 1.5 × 2.5 cm and cb exsolution lamellae larger than 1.5 × 15 mm. Irregular areas of cb several mm across may in part represent replacement of pn and are commonly associated with clusters of mt grains as much as 4 mm across. These mt grains may show several straight sides, but more typically show extremely irregular, rounded forms. Also identified: PtSn, PdBi, Pd_2Sn, Ag, PbTe, PbS.

90OMZS1-1: Oktyabr'sky mine, Shaft 1; massive tk–mh–cb–pn–mt ore. Tk and mh coexist in a fine exsolution texture, that in turn hosts cb exsolution lamellae smaller than 0.5 × 5 mm. Pn grains as large as 2 cm are veined by cb, which also forms irregular patches as much as 7 mm across. Mt occurs as partly euhedral, partly intricate grains as much as 8 mm across. Also identified: Pd_2Bi, Pd_3Sn, Ag, (Zn,Cd)S, PbS, valleriite.

90OC1: Oktyabr'sky mine, Bend 67, Part 5; collected near upper contact of the Kharaelakhsky orebody; disseminated cpy–pn ore in contact gabbrodolerite. Sulfide occurs as interstitial component (less than 5 mm across) into which euhedral plagioclase grains commonly project. Also identified: ZnS stars in cpy, PbSe, PbS.

90KMZ5: Komsomolosky mine, east orebody; nearly massive po–cpy–pn–mt ore. Cpy and gangue are interstitial to po lenses as much as 1 cm across. Pn occurs as two generations of exsolution lamellae in po and as irregular replacement borders as much as 0.08 mm thick around cpy in contact with po. Pn lamellae may broaden and extend from po host into gangue. Py, occasionally with euhedral cube faces as much as 0.2 mm across, is a component of the gangue.

90MC10: Medvezhy Creek open pit, classic po–cpy–pn droplet ore in picritic–taxitic gabbrodolerite (Fig. 5). Sulfide concentrations range from disseminations to droplets as large as 2 × 3.5 cm. Masses of po and pn (to 1 cm across) are concentrated in the lower part of each droplet, with areas of po relatively free of inclusions but containing sparse pn exsolution lamellae; areas of fractured pn contain sparse irregular residues(?) of po. Upper part of each droplet consists of a highly irregular intergrowth of po (<0.2 mm across) in cpy, which may contain fine cb lamellae (as thin as 0.01 mm, in bundles as much as 1 mm long). See figure and text for further discussion. No trace phases seen.

90MC16: Medvezhy Creek open pit; from massive cpy–cb–po–pn vein >20 cm wide. Irregular areas of po are less than 0.5 cm across. Textures among cpy, pn, and cb are complex. Cpy appears to be extensively replacing pn and in turn may contain a crystallographically controlled latticework of Fe-oxide lamellae. Massive and lamellar cb are also intergrown with cpy. Also identified: $PtAs_2$, PtTe, PdBiTe, PdNiAs, electrum.

90MC15: Medvezhy Creek open pit; from massive cpy–cb–pn vein. Cpy hosts subhedral pn grains (2–12 mm across) and herring-bone cb lamellae as large as 2 × 15 mm. Irregular patches of mk are abundant in pn (Fig. 6). Also identified: Pd–Pt alloy, PtPdSn, PdBi, PdBiTe, Pd_2As, Pd_2Pb, electrum.

90MCZC1: Medvezhy Creek open pit; from massive cpy–cb–pn vein >15 cm wide. Chains of pn grains (2–5 mm across, rarely 1 cm) surround areas as large as 2 × 6 cm composed predominantly of cpy hosting cb lamellae (typically <1 mm wide and 1.5 cm long). Mk occurs as abundant irregular patches in pn. Also identified: Pt–Fe alloy, PdBiTe, PdTe, electrum.

90MC5: Medvezhy Creek open pit; from massive cpy–pn vein. Cpy hosts pn grains as large as 1.5 cm across, that show minor (<0.1 mm across) alteration to mk. Pn also occurs as elongate crystals and lenses ~0.2 mm wide. Subhedral mt grains 0.5–2 mm across) lie within the vein against wallrock. Also identified: PdBiTe, PdAgTe, Pd_2Pb, (Zn,Cd)S stars in cpy.

839: High-grade reference-collection sample from 5–7 m below upper contact of the Kharaelakhsky orebody, near Shaft 2 of the Oktyabr'sky mine; massive cpy–pn–po–gal–cb ore from vein cutting primary pn–cpy ore. Cpy hosts pn grains as large as 4 × 10 mm, irregular elongated rounded patches of gal (as large as 1 × 10 mm), sparse cb in the form of irregular lamellae as wide as 0.5 mm but no longer than 2 mm, and elongate irregular stringers of po that may measure 1 mm across, but also may be 2 cm long and never more than 0.3 mm wide. Cpy, cb, and po are crowded with micrometric inclusions of PbS and PbTe. Sparse amoeboid mt grains may be 1.5 mm across. Also identified: PtBiTe, (Pt,Pd)BiTe, PtBiSb, PdBiTe, PdBi, Pd_2Sn, Bi, BiTe, AgTe, electrum.

90OC21: High-grade reference-collection sample from Oktyabr'sky mine, Shaft 2. Half of specimen is composed of silicates, corroded mt, and cpy in roughly equal proportions: portion 2 cm wide consists of complex cpy–gal intergrowth, which in part can be likened to a fingerprint in intricacy and scale. Subhedral $PtAs_2$ crystals 5 mm across occur 3 cm apart in this intergrowth. Sparse pn grains and areas of cb are smaller than 1 mm; pn shows patchy alteration to mk. Cpy and cb are crowded with micrometric grains of gal. Also identified: $PdBi_2$, (PdPt)BiTe.

90OC25: Reference-collection sample from Oktyabr'sky mine; bn vein 2 cm wide contains angular masses of cpy as much as 1.5 cm across and areas of Ni-rich pn as much as 1 cm across. In some areas, pn appears to be merely fractured and cut by bn veins, in others only small irregular residues of pn remain. Sparse grains of gd (<0.4 mm across) appear to have grown contemporaneously with bn against cpy. Also identified: ZnS stars in cpy.